Molecular Pharmacology Fast Forward. Published on November 2, 2011 as doi:10.1124/mol.111.074179

MOL #74179

Characterization of Mdr1a/P-glycoprotein knockout rats generated by zinc finger nucleases

Xiaoyan Chu, Zuo Zhang, Jocelyn Yabut, Sarah Horwitz, John Levorse, Xiang-qing Li, Lei Zhu, Harmony Lederman, Rachel Ortiga, John Strauss, Xiaofang Li, Karen A. Owens, Jasminka Dragovic, Thomas Vogt, Raymond Evers and Myung K. Shin

Pharmacokinetics, Pharmacodynamics and Drug Metabolism (PPDM) (XC, JY, XL, KAO, JD, RE), Genetically Engineered Model (GEM) (ZZ, SH, JL, XL, LZ, TV, MKS), Laboratory Animal Resources (HL), and Rahway Central Pharmacology (RO, JS), Merck & Co. & Inc. 126 E. Lincoln Avenue, PO Box 2000, Rahway, NJ, 07065, USA

Molecular Pharmacology Fast Forward. Published on November 2, 2011 as DOI: 10.1124/mol.111.074179
This article has not been copyedited and formatted. The final version may differ from this version.

Running title:

Mdr1a knockout rat

Correspondence should be addressed to:

Dr. Myung Kyun Shin

Merck Sharp & Dohme Corp., RY80Y-310

126 East Lincoln Avenue

Rahway, NJ 07065, USA

Tel +1 732 594 3230; Fax +1 732 594 5878

e-mail myung.shin2@merck.com

The document statistics

Number of text pages: 28 (excluding title and tables)

Number of tables: 1

Number of figures: 4

Number of references: 40

Number of words in Abstract: 199

Number of words in Introduction: 647

Number of words in Discussion: 963

Non standard abbreviations:

Zinc Finger Nuclease (ZFN), P-glycoprotein (P-gp), central nervous system (CNS) DNA double-strand break (DSB), non-homologous end joining (NHEJ), homologous recombination (HR), knockout (KO), area under the curve (AUC), clearance (CL)

Molecular Pharmacology Fast Forward. Published on November 2, 2011 as DOI: 10.1124/mol.111.074179
This article has not been copyedited and formatted. The final version may differ from this version.

Abstract

The development of the Zinc Finger Nuclease (ZFN) technology has enabled the genetic engineering of the rat genome. The ability to manipulate the rat genome has great promise to augment the utility of rats for biological and pharmacological studies. A Wistar Hannover rat model lacking the multidrug resistance protein Mdr1a P-glycoprotein (P-gp) was generated using a rat Mdr1a specific ZFN. Mdr1a was completely absent in some tissues, including brain and small intestine, of the knockout rat. Pharmacokinetic studies with the Mdr1a P-gp substrates loperamide, indinavir, and talinolol indicated that Mdr1a was functionally inactive in the blood-brain barrier and intestine in the Mdr1a$^{-/-}$ rats. To identify possible compensatory mechanisms in Mdr1a$^{-/-}$ rats, the expression level of 90 drug metabolizing enzyme and transporter related genes was compared in brain, liver, kidney and intestine of male and female Mdr1a$^{-/-}$ and control rats. In general, alterations in gene expression of these genes in Mdr1a$^{-/-}$ rats appeared to be modest, with more changes in female than in male rats. Taken together, our studies demonstrate that the ZFN generated Mdr1a$^{-/-}$ rat will be a valuable tool for central nervous system (CNS) drug target validation and determining the role of P-gp in drug absorption and disposition.

Molecular Pharmacology Fast Forward. Published on November 2, 2011 as DOI: 10.1124/mol.111.074179
This article has not been copyedited and formatted. The final version may differ from this version.

Introduction

The gene targeting technology using embryonic stem (ES) cells to modify specific alleles in mice has been an invaluable tool to increase the understanding of gene function and disease processes (Capecchi, 2005). However, its ability to specifically target and manipulate the genome of other species has been limited. Notwithstanding, several recent breakthroughs in manipulating the rat genome hold great promise in generating better animal models to study human disease (Hamra, 2010; Tong et al., 2010). The ability to generate genetically altered rat models would be particularly valuable in drug discovery as rats are frequently used as pharmacology models for pharmacokinetics and toxicity studies (Aitman et al., 2008).

One of these promising methods for generating genetically engineered rat models is the zinc finger nuclease (ZFN) technology. The ZFN is created by linking zinc finger DNA binding domains (Klug, 2010) to a Fok I nuclease domain. The engineered chimeric protein introduces a DNA double-strand break (DSB) at a predesigned genomic locus (Urnov et al., 2010), which is then repaired by the error-prone non-homologous end joining (NHEJ) pathway or the accurate homologous recombination (HR) pathway. The former mechanism results in small deletions or insertions near the repaired region, frequently leading to frame-shifts and the creation of a targeted knockout (KO) allele (Urnov et al., 2010). ZFN technology has been successfully used to generate targeted KO rat (Geurts et al., 2009) in a shorter time frame than ES cell based gene targeting (Le Provost et al., 2009), and has been applied in other species (Geurts and Moreno, 2010; Urnov et al., 2010).

Molecular Pharmacology Fast Forward. Published on November 2, 2011 as DOI: 10.1124/mol.111.074179
This article has not been copyedited and formatted. The final version may differ from this version.

P-glycoprotein (P-gp, ABCB1) is localized in the plasma membrane of cells where it mediates the ATP-dependent export of drugs (Eyal et al., 2009; Giacomini et al., 2010; Lee et al., 2010; Schinkel and Jonker, 2003). Human MDR1 was first discovered by its overexpression in multidrug resistant tumor cell lines (Juliano and Ling, 1976), but is also expressed in various tissues such as in the luminal membrane of the small intestine, the blood–brain barrier, the apical membrane of hepatocytes, and kidney proximal tubule epithelia (Kimura et al., 2007; Miller et al., 2008; Raub, 2006; Zhou, 2008). In the mouse and rat genome, there are two paralogous genes encoding P-gp: Mdr1a and Mdr1b, which amino acid sequences are 83% identical (Devault and Gros, 1990). Based on RNA analysis, mouse Mdr1a is predominantly expressed in intestine, brain, and testis, whereas the expression of Mdr1b is most prominent in the adrenal, ovaries, placenta, and kidneys. Both Mdr1a and Mdr1b are also expressed in liver and heart (Chen et al., 2003; Schinkel et al., 1994). P-gp has broad substrate specificity, most of which are neutral and amphipathic positively charged compounds, including many commonly prescribed drugs from various chemical and pharmacological classes (Lee et al., 2010; Mahar Doan et al., 2002; Zhou, 2008).

The Mdr1a$^{-/-}$ or Mdr1a/1b$^{-/-}$ mice, and Mdr1a deficient CF-1 mice have been widely used to assess the role of P-gp *in vivo* (Chen et al., 2003; Schinkel, 1998; Schinkel et al., 1996; Schinkel et al., 1995). For instance, *in vivo* studies in Mdr1a$^{-/-}$ mice have demonstrated the functional importance of P-gp in limiting brain penetration of many drugs, and have also established a role of Mdr1 in drug absorption, and excretion into bile and urine (Chen et al., 2003; Jonker et al., 1999; Schinkel, 1998; Schinkel et al., 1996; Schinkel et al., 1995). Mdr1a $^{-/-}$ mice are a powerful tool for selecting non-P-gp substrates

Molecular Pharmacology Fast Forward. Published on November 2, 2011 as DOI: 10.1124/mol.111.074179
This article has not been copyedited and formatted. The final version may differ from this version.

for central nervous system (CNS) targeted drugs and establishing PK/PD relationships. As rats are frequently used in the drug development process, a rat model lacking Mdr1a would serve as an additional valuable *in vivo* model.

In this study, we used ZFN technology, to manipulate the rat Mdr1a gene. The resulting Mdr1a $^{-/-}$ rats were molecularly and pharmacologically characterized. Our results suggest that the Mdr1a rat KO model would serve as a valuable *in vivo* model for pharmacological studies.

Molecular Pharmacology Fast Forward. Published on November 2, 2011 as DOI: 10.1124/mol.111.074179
This article has not been copyedited and formatted. The final version may differ from this version.

Materials and Methods

Animals

Mdr1a$^{-/-}$ and wild-type Wistar Hannover rats (10-12 week old) were used. Animals were kept in a temperature controlled environment with a 12 h light/12 h dark cycle and received food and water *ad libitum*. All animal handling was according to Animal Procedure Statements approved by the Merck Rahway Institutional Animal Care and Use Committee.

Chemicals

Loperamide and indinavir were obtained from Sigma-Aldrich (St. Louis, MO). Talinolol was purchased from Toronto Research Chemicals (North York, Ontario). All other reagents were commercially obtained with the highest analytical purity grade.

ZFN mRNA preparation and microinjections of rat embryos

ZFN constructs targeting rat Mdr1a gene were designed and purchased from Sigma Aldrich. The constructs have been described elsewhere (Carbery et al., 2010; Cui et al., 2010) and the targeting site is listed in Figure 1. ZFN expression plasmids were linearized by XbaI site and transcribed using MessageMax T7 kit and poly(A) tailing kit (Epicentre, Madison, WI) according to the manufacturer's protocol. The final products were purified using MegaClean kit (Ambion, Austin, TX) and dissolved in water. RNA was quantified and adjusted to desired concentration (2ng/µl) using TE buffer (10mM Tris, pH7.6, 1mM EDTA) for embryo injection.

All animal work was done in accordance with Merck Institutional Animal Care guidelines. Wistar-Hannover rats purchased from Charles River Labs (Boston, MA) were housed in standard conditions under a 14 hour light 10 hour dark cycle. 4-5 week

Molecular Pharmacology Fast Forward. Published on November 2, 2011 as DOI: 10.1124/mol.111.074179
This article has not been copyedited and formatted. The final version may differ from this version.

old females were superovulated with 30 U PMSG followed 48 hours later by 40 U hCG and placed with fertile males of the same strain. Fertilized oocytes were collected the next morning and microinjected with ZFN mRNA (2 ng/µl) into cytoplasm or pronucleus. Surviving oocytes were implanted into the oviducts of pseudopregnant Sprague Dawley females and allowed to go to term.

Genomic DNA preparation and targeted allele identification

Rat genomic DNA was extracted from the tail tip using the Mammalian GenElute kit (Sigma, St. Louis, MO) following the manufacturer's protocol. To detect small deletions generated by NHEJ, a Cel-1 assay was performed as described elsewhere using the Surveyor mutation detection kit (Carbery et al., 2010). The sequences of PCR primers of Mdr1a are TTGGCAAAACAAAACTGGCT and TTAGCAAAAAGCATGAAATTGTG.

Western blot analysis

Rat tissue samples were collected and snap-frozen in liquid nitrogen for future processing. Membrane fractions from different tissues were prepared using Qproteome cell compartment kit (Qiagen, Hilden, Germany) following manufacturer's protocol. 20-30 µg of protein for each sample was loaded onto NuPage 4-12% SDS gel (Invitrogen, Carlsbad, CA) and transferred to nitrocellulose membrane. Western blot using anti-Mdr1a (C219, Abcam) or anti-Actin (Cell Signaling) antibodies was carried out using WesternBreeze chemiluminescent kit (Invitrogen) following the manufacturer's protocol.

Analysis of serum and urine

Male and female Mdr1a$^{-/-}$ and wild type rats were used in this study. The animals were fasted overnight with free access to water before the study. Blood samples were

Molecular Pharmacology Fast Forward. Published on November 2, 2011 as DOI: 10.1124/mol.111.074179
This article has not been copyedited and formatted. The final version may differ from this version.

taken by cardiac puncture. The serum samples obtained were used for analysis. Urine samples were collected overnight in metabolic cages. During urine collection, samples were kept on ice and in the dark. Serum and urine chemistry parameters were determined using a Hitachi 911 clinical chemistry analyzer (Roche Diagnostics, Indianapolis, IN). Sodium, potassium and chloride levels were determined using ion-specific electrodes. Other tests were performed by standard biochemical methods.

Loperamide and indinavir brain penetration studies

Male Mdr1a$^{-/-}$ and wild-type rats were used in these studies. Loperamide was dissolved in saline containing 5% ethanol at a concentration of 0.2 mg/mL. Indinavir was dissolved in saline: propylene glycol: ethanol (50:40:10, v/v) at a concentration of 0.5 mg/mL. After intravenous administration of loperamide (1 mg/kg) or indinavir (2mg/kg) via catheterized femoral vein, three rats from each group were sacrificed at 0.5, 2, and 4hr, and plasma and brain samples were collected. All samples were kept at –80°C until LC-MS/MS analysis.

Talinolol pharmacokinetic studies

Male Mdr1a$^{-/-}$ and wild-type rats were used in these studies. The animals were fasted overnight with free access to water before the study. Talinolol, formulated in sodium phosphate buffer (0.2M, pH 7.4): propylene glycol : ethanol (40:40:20, v/v) or polyethylene glycol 400 : ethanol : water (25:15:60, v/v), was administered via intravenous injection into catheterized femoral vein (1mg/kg) or oral gavage (5mg/kg). Multiple blood samples were collected from the femoral artery at designated time points and plasma samples were separated by centrifugation immediately. All samples were kept at -80^{o}C until further analysis.

Molecular Pharmacology Fast Forward. Published on November 2, 2011 as DOI: 10.1124/mol.111.074179
This article has not been copyedited and formatted. The final version may differ from this version.

Quantitative RT-PCR and PCR array for mRNA analysis

RNA was isolated from tissues of Mdr1a $^{-/-}$ and wild-type male and female rats with three animals per group. Total RNA was isolated using the RNeasy kit from Qiagen, and cDNA was synthesized using High-Capacity cDNA Archive kit (Applied Biosystems, Foster City, CA) as described previously (Chu et al., 2006). Taqman low-density microarrays (TLDA) cards were custom made by Applied Biosystems and contained probes for the detection of 90 genes (supplementary table 1 and 2). Real-time quantitative PCR was performed using an ABI PRISM 7900 Sequence Detection System (Applied Biosystems). Changes in gene expression were determined by the ΔΔCt method (Livak and Schmittgen, 2001). The cycle threshold value (Ct) represents the PCR cycle at which the level of fluorescence during RT-PCR for a specific target gene exceeds the baseline threshold. Quantitation of the target cDNAs in all samples were normalized to 18S ribosomal RNA ($Ct_{target} - Ct_{18S} = \Delta Ct$), and the difference in expression for each target cDNA in the Mdr1a $^{-/-}$ rat was expressed to the amount in the wild-type rat ($\Delta Ct_{wild\text{-}type} - \Delta Ct_{Mdr1a\ -/-} = \Delta\Delta Ct$). Fold changes in target gene expression were determined by taking 2 to the power of this value ($2^{-\Delta\Delta Ct}$).

A 384-well format custom designed PCR array was ordered from SABiosciences-Qiagen. The custom rat 384-well array was designed to combine four existing SABioscience's 96-well arrays for Drug Metabolism and Transporters (Drug Metabolism: Phase I Enzymes, Drug Metabolism: Phase II Enzymes, Drug transporters, and Drug Resistance & Metabolism PCR Array (http://www.sabiosciences.com/ArrayList.php?pline=PCRArray). A total of 372 genes and 5 house keeping genes were assayed. Genomic DNA Contamination primer control

Molecular Pharmacology Fast Forward. Published on November 2, 2011 as DOI: 10.1124/mol.111.074179
This article has not been copyedited and formatted. The final version may differ from this version.

and positive PCR controls were all included on the array as part of SABiosciences standard array setup. 0.5-2 µg total RNA from each sample was used in 50 µl cDNA reaction by using high capacity archive cDNA kit (Applied Biosystems, Foster City, CA). cDNA reaction was setup in Biomek FX liquid handling system. 10 µl of the PCR reaction was loaded into each well of the PCR array using Biomek FX liquid handling system. Real-time PCR was performed on the 7900HT PCR System (Applied Biosystems, Foster City, CA) with 2x SYBR Fast PCR Master Mix (SABioscienses-Qiagen) and 2 µl cDNA for each reaction. The expression levels of mRNA for each gene were normalized to the average of Actb, Hprt1, Ldha, Rplp1 and Rp113a in each sample. Genes with greater than 2-fold changes were further validated by individual Taqman (ABI) qRT-PCR.

Quantification of loperamide, indinavir, and talinolol in plasma and brain samples

Plasma samples were thawed on ice. A 50 microliter sample was taken and six volumes of acetonitrile containing 100 nM of Alprazolam or 40ng/mL of labetolol (Sigma-Aldrich, St. Louis, MO) as internal standard were added to the samples and standard solutions. After mixing, the contents were centrifuged at 1800g for 10 min. The supernatant was then transferred to a 96-well plate and analyzed using liquid chromatography-tandem mass spectrometry. Brain samples were weighed, placed in a 20-well plate and a two-fold amount of water, and four stainless steel beads were added. The brains were then homogenized using the 2000 Geno/Grinder (Spex CertiPrep). A 100-150 microliter sample of the homogenate of each brain sample was taken and placed in a 96-well plate and analyzed by LC/MS/MS. Chromatography was performed using an Atlantis T3, 2.1x50 mm, 3 micron particle size, (Waters, Part no. 186003717) and an HPLC system consisting of Thermo Scientific Transcend System pumps and Thermo

Molecular Pharmacology Fast Forward. Published on November 2, 2011 as DOI: 10.1124/mol.111.074179
This article has not been copyedited and formatted. The final version may differ from this version.

Scientific LX-2 (with Aria OS 1.61 operating system) autosampler, using a gradient of water with 0.1% formic acid (A) and acetonitrile with 0.1% formic acid (B). The HPLC flow rate was 0.7 to 0.75 mL/min. Before the gradient was begun, the mobile phase was 5% B for 15 seconds. The gradient was then started with 5 or 10% B going to 90 or 95% B over 60 or 90 seconds. The mobile phase was then 90 or 95% B for 25 seconds after which it was returned to 5 or 10% B for 50 or 60 seconds. Detection of the loperamide and talinolol was performed using a Sciex API 5000 mass spectrometer (MDS-Sciex, Toronto, ON, Canada), and indinavir using a Sciex API 4000 mass spectrometer (MDS-Sciex, Toronto, ON, Canada) in the positive ion mode using the Turbo-Ion Spray source. Mass transition (m/z) monitoring for the loperamide, talinolol, and indinavir was 477.2 to 266.2, 364.1 to 100.4, and 614.2 to 465.4, respectively. The concentration of test compound in plasma or brain samples was determined by comparing the test compound to internal standard peak area ratios against a standard curve. Lower limit of quantification in both matrices was 0.5ng/mL (talinolol) and 1ng/mL (loperamide). All quality controls were within 20-25% of nominal value.

Determination of pharmacokinetic parameters

Pharmacokinetic parameters of talinolol were calculated using Watson software (version 6; Watson Software System) with non-compartmental models.

Statistical analysis

Student t-Tests were used to determine the significance of differences between groups of animals. Differences with P values <0.05 were considered significant.

Molecular Pharmacology Fast Forward. Published on November 2, 2011 as DOI: 10.1124/mol.111.074179
This article has not been copyedited and formatted. The final version may differ from this version.

Results

Generation of Mdr1a KO rats using a sequence specific ZFN

A pair of ZFNs was designed and generated by Sigma Aldrich to target the rat Mdr1a gene (Carbery et al., 2010; Cui et al., 2010). The ZFN target site resides in Mdr1a exon 7 (Figure 1A). The ZFN was initially tested in rat C6 cells (supplementary Figure s1), showing that it specifically targeted the Mdr1a gene with high efficiency, but not the closely related Mdr1b gene. To test the ZFN activity in rats, the mRNAs encoding Mdr1a ZFNs were directly injected into the pro-nuclei or cytoplasm of one-cell embryos. The resulting pups were genotyped by the Cel-1 assay or direct PCR using genomic DNA isolated from tails. As shown in Figure 1B, two pups out of seven contained mutations near the ZFN target site. The mutant alleles from the two founders were cloned and sequenced. Interestingly, multiple mutant alleles were identified in these founders including four in founder 6 and three in founder 7 (Figure 1B). This mosaic nature of the founders generated by ZFN is consistent with previous reports (Carbery et al., 2010; Cui et al., 2010; Geurts et al., 2009; Mashimo et al., 2010), and suggests that the activity of the ZFN can persist beyond the one cell stage of embryogenesis. Among the 66 live-born off-spring, 22 (~33%) positive founders carrying mutant alleles were identified (supplementary Table s1). Moreover, analyses of rat genomic regions that shared high homology (with 4 or 5 mismatches) to the Mdr1a ZFN site did not detect any off-target cleavage (supplementary Figure s2).

Mdr1a$^{-/-}$ rats displayed normal development, viability, and fertility, without obvious differences from wild-type rats in terms of body weight and fecal matter. In general, serum and urine chemistry parameters in Mdr1a$^{-/-}$ rats were comparable with

Molecular Pharmacology Fast Forward. Published on November 2, 2011 as DOI: 10.1124/mol.111.074179
This article has not been copyedited and formatted. The final version may differ from this version.

those in controls, except for a 2.2-fold lower urine calcium level in male KO compared to wild-type, a 1.7-fold higher urine calcium level in female KO compared to wild-type, as well as a 3.5-fold lower urine protein level in KO female compared to wild-type animals (data not shown).

Detection of Mdr1 by Western blotting

To confirm that the ZFN generated mutations resulted in non detectable levels of the Mdr1a protein, we characterized the homozygous Mdr1a$^{-/-}$ rats by Western blotting. Membrane fractions from wild-type and Mdr1a$^{-/-}$ rat brain, small intestine, liver and kidney were analyzed using the anti-Mdr1a antibody C219. Two KO rats were examined. KO1 carries two identical 19bp deletion alleles. KO2 carries one 19bp deletion and one 428bp deletion alleles. As shown in Figure 1C, the Mdr1a protein was completely absent in both brain and small intestines of the two Mdr1a$^{-/-}$ rat strains analyzed. Since C219 also cross-reacts with Mdr1b, the Western blots demonstrated that Mdr1b expression was still present in liver and kidney. This was especially the case in liver where Mdr1b is likely up-regulated upon inactivation of the Mdr1a gene (see below and Figure 1C). As no difference between the two deletion alleles (19bp and 428bp) characterized was detected, all subsequent studies were conducted using the homozygous strain with the 19 bp deletion in Mdr1a exon 7.

Brain penetration of loperamide and indinavir in *Mdr1a*$^{-/-}$ rats

To confirm the functional absence of Mdr1a in Mdr1a$^{-/-}$ rats, brain penetration of loperamide and indinavir, two previously validated substrates for human MDR1 and rodent Mdr1a (Choo et al., 2000; Kim et al., 1998; Schinkel et al., 1996), were investigated in Mdr1a$^{-/-}$ and wild-type rats. After intravenous (i.v.) administration of

Molecular Pharmacology Fast Forward. Published on November 2, 2011 as DOI: 10.1124/mol.111.074179
This article has not been copyedited and formatted. The final version may differ from this version.

loperamide, the brain concentration of loperamide in Mdr1a$^{-/-}$ rats was 22- to 107-fold (at 0.5, 2, and 4hr, $p<0.05$), higher than in control rats (Figure 2A), whereas the plasma concentration time profile of loperamide in Mdr1a$^{-/-}$ rats was 1.3- to 2-fold higher than in wild-type rats (at 0.5, 2, and 4hr, $P<0.05$) (Figure 2B). The brain-to-plasma concentration ratio ($K_{p, brain}$) in wild-type rats ranged from 0.36 to 0.42, while the ratio in Mdr1a$^{-/-}$ rats was time-dependent and increased from 7- to 23-fold (at 0.5, 2, and 4hr, $P<0.05$,) (Figure 2C), indicating a loss of function of Mdr1a in the brain of Mdr1a$^{-/-}$ rats. Furthermore, as loperamide is an opioid-receptor agonist, pronounced opiate-like CNS effect were observed in the Mdr1a$^{-/-}$ rats, such as weak breathing, immobility, and no blink reflex. Similar to loperamide, the indinavir brain concentration in Mdr1a$^{-/-}$ rats was significantly higher than in wild-type rats at all time points tested ($p<0.05$), (Figure 2D), while there was no significant difference in the plasma concentration time profile (Figure 2E). The $K_{p, brain}$ of indinavir in wild-type rats was time dependent and increased from 0.5 to 2.6, while $K_{p, brain}$ in Mdr1a$^{-/-}$ rats increased from 6.4 to 77.2 (at 0.5 and 2h, $p <0.05$) (Figure 2F).

Pharmacokinetics of talinolol in Mdr1a$^{-/-}$ rats

To assess the effect of Mdr1a on the intestinal absorption and pharmacokinetics of talinolol, a substrate for human and rat P-gp and organic anion transporting polypeptides (OATPs) (Shirasaka et al., 2010; Shirasaka et al., 2009), we administered talinolol orally or i.v. to wild-type and Mdr1a$^{-/-}$ rats, and subsequently determined the plasma concentration-time profile (Figure 3A, 3B). Analysis of the pharmacokinetic parameters showed that the area under the curve ($AUC_{0-\infty}$) and plasma clearance (CL) in Mdr1a$^{-/-}$ was comparable with that in wild-type rats following intravenous administration, whereas

Molecular Pharmacology Fast Forward. Published on November 2, 2011 as DOI: 10.1124/mol.111.074179
This article has not been copyedited and formatted. The final version may differ from this version.

the $AUC_{0-\infty}$ in Mdr1a$^{-/-}$ rats was increased 4.5-fold ($P<0.05$) after oral administration (Table 1). The bioavailability (F %) of talinolol in Mdr1a$^{-/-}$ and wild-type rats was 23% and 7%, respectively (Table 1).

Gene expression profiling in brain, intestine, liver, and kidney

To investigate if the loss of Mdr1a alters the expression profile of other drug transporters and metabolizing enzymes, we used 96-well TaqMan Low-Density Microarrays (Microfluidic Cards) and 384-well PCR arrays (Qiagen-SABiosciences) to determine the expression changes in brain, intestine, liver, and kidney of wild-type and Mdr1a$^{-/-}$ female and male rats. The genes in the 384-well PCR array included the ninety Phase I and II drug metabolizing enzymes and transporters in the Taqman Low-Density array as well as additional 282 Drug metabolism and transporter genes (Tables S2-4). The genes with significant changes observed from the 372-gene panel (Table S2-3 and Figure S3) were further validated by individual Taqman qRT-PCR. The genes which showed ≥ 2-fold up- or down- regulation ($P<0.05$), based on Taqman qRT-PCR, in Mdr1a$^{-/-}$ rats compared to wild-type animals in liver, intestine, kidney, and brain is presented in Figure 4.

The amount of Mdr1a *(Abcb1a)* mRNA was 5-50-fold lower in brain, liver, kidney and intestine of Mdr1a$^{-/-}$ rats than wild-type rats. Lower transcript level of Mdr1a mRNA likely resulted from nonsense-mediated mRNA decay as the deletion in exon 7 caused the generation of multiple downstream premature termination codons. Similar to a previous report in Mdr1a$^{-/-}$/1b$^{-/-}$ mice (Shinkel., 1997), Mdr1b (*Abcb1b*) gene expression was low in brain and intestine of both Mdr1a$^{-/-}$ and wild-type rats. Interestingly, Mdr1b was 4.7-fold higher and 2-fold lower in the liver of male and female Mdr1a$^{-/-}$ rats,

Molecular Pharmacology Fast Forward. Published on November 2, 2011 as DOI: 10.1124/mol.111.074179
This article has not been copyedited and formatted. The final version may differ from this version.

respectively, whereas its expression in kidney of both male and female Mdr1a$^{-/-}$ rats was not changed compared to controls. In female, but not in male Mdr1a$^{-/-}$ rats, a 2-fold up-regulation of Mrp5 (*Abcc5*) in brain, and a 2-2.5-fold lower expression of *Abcg1*, Oct1 (*Slc22a1*), and Bcrp (*Abcg2*) in intestine was observed. In addition, *Abcg5* and *Abcg8* in liver of female Mdr1a$^{-/-}$ rats was 2.5-3-fold lower than in wild-type animals. No significant differences were detected for any of the other transporter genes analyzed.

Of the Cytochrome P450 and nuclear receptor genes analyzed, the expression of Cyp3a1/Cyp3a23 in liver of both male and female Mdr1a$^{-/-}$ rats was not changed compared to wild-type rats. In female Mdr1a$^{-/-}$ liver, the expression of Cyp1a2, Cyp2b2, Cyp2d4v1, Cyp3a18, Cyp4a1 and the constitutive androstane receptor (Car, Nr1i3) was 2.5-5-fold lower than in controls, while Cyp7a1 was 3-fold higher than in controls. In male Mdr1a$^{-/-}$ liver, Cyp26a1 and Cyp4a1 were expressed 2.5-fold lower and 2-fold higher than in wild-type rats, respectively. The Cyp3a9 and Cyp3a62 enzymes, which contribute to intestinal drug metabolism in rats (Aiba et al., 2005), were 3-fold lower in female Mdr1a$^{-/-}$. The expression of Cyp2d1 was 3-5-fold lower in both male and female intestine of Mdr1a$^{-/-}$ rats. In kidney, expression of Cyp1a1 and Cyp26b1 was 2.5-3-fold lower in male and female Mdr1a$^{-/-}$ rats, respectively.

For the UDP-glucuronosyltransferase (UGT) and sulfotransferase (SULT) genes analyzed, Sult1a1 was 3-fold lower in the intestine of male Mdr1a$^{-/-}$ rats. Ugt1a7c was 5-fold lower in kidney of female Mdr1a$^{-/-}$ rats. The 3.7 fold up-regulation of Cdkn1a (cyclin-dependent kinase inhibitor 1) gene was observed in male Mdr1a$^{-/-}$ rat.

Molecular Pharmacology Fast Forward. Published on November 2, 2011 as DOI: 10.1124/mol.111.074179
This article has not been copyedited and formatted. The final version may differ from this version.

Discussion

We have generated an Mdr1a$^{-/-}$ rat model using ZFN-mediated gene targeting through NHEJ pathways with high efficiency. The Mdr1a$^{-/-}$ rats are healthy and show no obvious phenotypic abnormalities. Western blots confirmed that no Mdr1a was present in brain and intestine. A signal was still detectable in kidney and liver, explained by the cross reactivity of the antibody used with Mdr1b. The functional absence of Mdr1a was demonstrated by a significant increase in brain penetration of loperamide and indinavir and the intestinal absorption of talinolol in the Mdr1a$^{-/-}$ rats.

A general concern in the use of transporter knockout animals for pharmacokinetic studies is the potential compensatory effect from up/down-regulation of other transporters and drug metabolism-related genes which may complicate the interpretation of data obtained with such animals. As reported by Schinkel et al. in Mdr1a$^{-/-}$ mice (Schinkel et al., 1994), the expression of Mdr1b was higher in the liver of male and female mice, and the kidney of male mice as well. Our studies showed that Mdr1b RNA was up-regulated 4.7-fold only in the liver of male Mdr1a$^{-/-}$ rats, whereas the expression of Mdr1b in kidney of both male and female Mdr1a$^{-/-}$ rats was unchanged. Since the anti-Mdr1a antibody used in Western blot analysis cross-reacts with the Mdr1b protein, high expression of Mdr1 detected in the male Mdr1a$^{-/-}$ liver is likely due to the up-regulation of Mdr1b. In the intestine of female Mdr1a$^{-/-}$ rats, the expression of Bcrp, which may contribute to intestinal secretion of its substrates, was ~50% lower compared to that in wild-type animals. However, it is not clear if such changes at the level of mRNA levels will translate into the change at the Bcrp protein level. We were not able to test this by

Molecular Pharmacology Fast Forward. Published on November 2, 2011 as DOI: 10.1124/mol.111.074179
This article has not been copyedited and formatted. The final version may differ from this version.

Western blot analysis due to unavailability of very selective Bcrp antibodies (data not shown).

In general, alterations in gene expression of phase I and II drug metabolizing enzymes in Mdr1a$^{-/-}$ rats appeared to be modest, with more changes in female rats. For instance, hepatic expression of Car, one of major nuclear receptors responsible for regulating many ADME related genes was 5-fold lower in female Mdr1a$^{-/-}$ rats. The mechanism for such down-regulation is not clear. Numerous studies have suggested that CYP3A and P-gp work synergistically in limiting the systematic exposure of orally administered drugs (Benet et al., 1999). In female Mdr1a$^{-/-}$ rats, the mRNA expression of Cyp3a9 and Cyp3a62 in intestine was 3-fold lower than in wild-type rats. Although further studies are needed to confirm that these changes are resulting in altered enzyme activity, caution should be taken in interpreting pharmacokinetic data obtained in female Mdr1a$^{-/-}$ rats that are substrates for Cyp3a9 or Cyp3a62.

One of the major applications of Mdr1a$^{-/-}$ rats will be studying the role of P-gp in brain penetration of drugs, which has been critical for selecting CNS targeted drugs or reducing CNS toxicity for non-CNS drugs. Our findings demonstrate that Mdr1a$^{-/-}$ rats are a sensitive model to measure the role of P-gp in brain penetration. Similar to the reports in Mdr1a$^{-/-}$ mice (Schinkel et al., 1996; Kim et al., 1998), a significant increase in the brain penetration of loperamide and indinavir was observed in Mdr1a$^{-/-}$ rats. The ratio of $K_{p,\,brain}$ in KO vs. wild-type rats was 17 to 63-fold for loperamide and 9 to 30-fold for indinavir, respectively. This is higher than previously reported for Mdr1a$^{-/-}$ mice. The cause of this discrepancy is possibly due to the difference of analytical methods applied, as we measured $K_{p,\,brain}$ of the parent drugs loperamide or indinavir by LC-MS/MS, while

Molecular Pharmacology Fast Forward. Published on November 2, 2011 as DOI: 10.1124/mol.111.074179
This article has not been copyedited and formatted. The final version may differ from this version.

only total radioactivity was measured in the experiments with Mdr1a$^{-/-}$ mice. Alternatively, it cannot be ruled out that the activity of P-gp in the brain of rat is higher than in mouse.

In addition to brain penetration, Mdr1a$^{-/-}$ rats will be a useful tool to study the role of P-gp in limiting intestinal drug absorption. Talinolol, a clinically used β1 selective adrenergic antagonist, is a substrate for P-gp and OATPs (Shirasaka et al., 2009; 2010), and is not metabolized by CYP3A4. The overall metabolic clearance of talinolol is low, and 99% of the drug is eliminated unchanged (Trausch et al., 1995). The pharmacokinetics of talinolol after oral administration are nonlinear, and the extent of absorption is highly dependent on the dose level (Kagan et al., 2010), which might be attributed to saturation of P-gp-mediated intestinal efflux. Our studies showed that the plasma AUC of talinolol in Mdr1a$^{-/-}$ rats increased 4.5-fold compared to wild-type animals following oral administration (5 mg/kg), while P-gp did not have a significant effect on the plasma AUC of talinolol after intravenous dosing. Therefore, these data suggest that rat Mdr1a plays a significant role in limiting the intestinal absorption of talinolol. Interestingly, the oral bioavailability of talinolol in humans is much higher than in rats (~55% in humans at 100 mg dose vs. 7% in rats at 5 mg/kg) although the dose level in rats in our study was higher than in humans (Trausch et al., 1995). This is likely due to potential species differences in the functional activity of MDR1/Mdr1a and OATPs between human and rats. Further investigations are needed to confirm this hypothesis.

ZFN mediated direct gene KO in rat embryos has recently been proven to be successful in numerous reports (Geurts et al., 2010; Mashimo et al., 2010; Menoret et al.,

Molecular Pharmacology Fast Forward. Published on November 2, 2011 as DOI: 10.1124/mol.111.074179
This article has not been copyedited and formatted. The final version may differ from this version.

2010). However, genetic modification of target genes through homologous recombination (HR) is critical to enable engineering of the rat genome in a flexible way. A recent report has demonstrated the feasibility of achieving HR directly in rat embryo facilitated by ZFN (Cui et al., 2010). It may expand the application of this technology and allow the generation of conditional KO/KI or humanized rat models. The robustness and full utility of this advancement needs to be explored further.

Molecular Pharmacology Fast Forward. Published on November 2, 2011 as DOI: 10.1124/mol.111.074179
This article has not been copyedited and formatted. The final version may differ from this version.

Acknowledgement

We would like to thank Xiaoli Ping, Loise Gichuru, Nina Jochnowitz, Chris Loewrigkeit, Carol Ann Keohane and Alexandra Wickham for providing surgical support. Thanks to Irene Capodanno, Christian N. Nunes, and Pan Yi for technical assistance. We would also like to thank Merck Research Laboratories New Technology Review and Licensing Committee (NT-RLC).

Authorship Contributions

Participated in research design: Chu, Zhang, Vogt, Evers and Shin.

Conducted experiments: Chu, Zhang, Yabut, Horwitz, Levorse, Li, Zhu, Lederman, Ortiga, Strauss, Li, Owens, Dragovic

Performed data analysis: Chu, Zhang, Yabut, Evers and Shin.

Wrote or contributed to the writing of the manuscript: Chu, Zhang, Vogt, Evers and Shin

Molecular Pharmacology Fast Forward. Published on November 2, 2011 as DOI: 10.1124/mol.111.074179
This article has not been copyedited and formatted. The final version may differ from this version.

References

Aiba T, Yoshinaga M, Ishida K, Takehara Y and Hashimoto Y (2005) Intestinal expression and metabolic activity of the CYP3A subfamily in female rats. *Biol Pharm Bull* **28**(2):311-315.

Aitman TJ, Critser JK, Cuppen E, Dominiczak A, Fernandez-Suarez XM, Flint J, Gauguier D, Geurts AM, Gould M, Harris PC, Holmdahl R, Hubner N, Izsvak Z, Jacob HJ, Kuramoto T, Kwitek AE, Marrone A, Mashimo T, Moreno C, Mullins J, Mullins L, Olsson T, Pravenec M, Riley L, Saar K, Serikawa T, Shull JD, Szpirer C, Twigger SN, Voigt B and Worley K (2008) Progress and prospects in rat genetics: a community view. *Nat Genet* **40**(5):516-522.

Benet LZ, Izumi T, Zhang Y, Silverman JA and Wacher VJ (1999) Intestinal MDR transport proteins and P-450 enzymes as barriers to oral drug delivery. *J Control Release* **62**(1-2):25-31.

Capecchi MR (2005) Gene targeting in mice: functional analysis of the mammalian genome for the twenty-first century. *Nat Rev Genet* **6**(6):507-512.

Carbery ID, Ji D, Harrington A, Brown V, Weinstein EJ, Liaw L and Cui X (2010) Targeted genome modification in mice using zinc-finger nucleases. *Genetics* **186**(2):451-459.

Chen C, Liu X and Smith BJ (2003) Utility of Mdr1-gene deficient mice in assessing the impact of P-glycoprotein on pharmacokinetics and pharmacodynamics in drug discovery and development. *Curr Drug Metab* **4**(4):272-291.

Choo EF, Leake B, Wandel C, Imamura H, Wood AJ, Wilkinson GR and Kim RB (2000) Pharmacological inhibition of P-glycoprotein transport enhances the distribution of HIV-1 protease inhibitors into brain and testes. *Drug Metab Dispos* **28**(6):655-660.

Chu XY, Strauss JR, Mariano MA, Li J, Newton DJ, Cai X, Wang RW, Yabut J, Hartley DP, Evans DC and Evers R (2006) Characterization of mice lacking the multidrug resistance protein MRP2 (ABCC2). *J Pharmacol Exp Ther* **317**(2):579-589.

Cui X, Ji D, Fisher DA, Wu Y, Briner DM and Weinstein EJ (2010) Targeted integration in rat and mouse embryos with zinc-finger nucleases. *Nat Biotechnol.*

Devault A and Gros P (1990) Two members of the mouse mdr gene family confer multidrug resistance with overlapping but distinct drug specificities. *Mol Cell Biol* **10**(4):1652-1663.

Eyal S, Hsiao P and Unadkat JD (2009) Drug interactions at the blood-brain barrier: fact or fantasy? *Pharmacol Ther* **123**(1):80-104.

Geurts AM, Cost GJ, Freyvert Y, Zeitler B, Miller JC, Choi VM, Jenkins SS, Wood A, Cui X, Meng X, Vincent A, Lam S, Michalkiewicz M, Schilling R, Foeckler J, Kalloway S, Weiler H, Menoret S, Anegon I, Davis GD, Zhang L, Rebar EJ, Gregory PD, Urnov FD, Jacob HJ and Buelow R (2009) Knockout rats via embryo microinjection of zinc-finger nucleases. *Science* **325**(5939):433.

Geurts AM, Cost GJ, Remy S, Cui X, Tesson L, Usal C, Menoret S, Jacob HJ, Anegon I and Buelow R (2010) Generation of gene-specific mutated rats using zinc-finger nucleases. *Methods Mol Biol* **597**:211-225.

Geurts AM and Moreno C (2010) Zinc-finger nucleases: new strategies to target the rat genome. *Clin Sci (Lond)* **119**(8):303-311.

Molecular Pharmacology Fast Forward. Published on November 2, 2011 as DOI: 10.1124/mol.111.074179
This article has not been copyedited and formatted. The final version may differ from this version.

Giacomini KM, Huang SM, Tweedie DJ, Benet LZ, Brouwer KL, Chu X, Dahlin A, Evers R, Fischer V, Hillgren KM, Hoffmaster KA, Ishikawa T, Keppler D, Kim RB, Lee CA, Niemi M, Polli JW, Sugiyama Y, Swaan PW, Ware JA, Wright SH, Yee SW, Zamek-Gliszczynski MJ and Zhang L (2010) Membrane transporters in drug development. *Nat Rev Drug Discov* **9**(3):215-236.

Hamra FK (2010) Gene targeting: Enter the rat. *Nature* **467**(7312):161-163.

Jonker JW, Wagenaar E, van Deemter L, Gottschlich R, Bender HM, Dasenbrock J and Schinkel AH (1999) Role of blood-brain barrier P-glycoprotein in limiting brain accumulation and sedative side-effects of asimadoline, a peripherally acting analgaesic drug. *Br J Pharmacol* **127**(1):43-50.

Juliano RL and Ling V (1976) A surface glycoprotein modulating drug permeability in Chinese hamster ovary cell mutants. *Biochim Biophys Acta* **455**(1):152-162.

Kagan L, Dreifinger T, Mager DE and Hoffman A (2010) Role of p-glycoprotein in region-specific gastrointestinal absorption of talinolol in rats. *Drug Metab Dispos* **38**(9):1560-1566.

Kim RB, Fromm MF, Wandel C, Leake B, Wood AJ, Roden DM and Wilkinson GR (1998) The drug transporter P-glycoprotein limits oral absorption and brain entry of HIV-1 protease inhibitors. *J Clin Invest* **101**(2):289-294.

Kimura Y, Morita SY, Matsuo M and Ueda K (2007) Mechanism of multidrug recognition by MDR1/ABCB1. *Cancer Sci* **98**(9):1303-1310.

Klug A (2010) The discovery of zinc fingers and their applications in gene regulation and genome manipulation. *Annu Rev Biochem* **79**:213-231.

Le Provost F, Lillico S, Passet B, Young R, Whitelaw B and Vilotte JL (2009) Zinc finger nuclease technology heralds a new era in mammalian transgenesis. *Trends Biotechnol* **28**(3):134-141.

Lee CA, Cook JA, Reyner EL and Smith DA (2010) P-glycoprotein related drug interactions: clinical importance and a consideration of disease states. *Expert Opin Drug Metab Toxicol* **6**(5):603-619.

Livak KJ and Schmittgen TD (2001) Analysis of relative gene expression data using real-time quantitative PCR and the 2(-Delta Delta C(T)) Method. *Methods* **25**(4):402-408.

Mahar Doan KM, Humphreys JE, Webster LO, Wring SA, Shampine LJ, Serabjit-Singh CJ, Adkison KK and Polli JW (2002) Passive permeability and P-glycoprotein-mediated efflux differentiate central nervous system (CNS) and non-CNS marketed drugs. *J Pharmacol Exp Ther* **303**(3):1029-1037.

Mashimo T, Takizawa A, Voigt B, Yoshimi K, Hiai H, Kuramoto T and Serikawa T (2010) Generation of knockout rats with X-linked severe combined immunodeficiency (X-SCID) using zinc-finger nucleases. *PLoS One* **5**(1):e8870.

Menoret S, Iscache AL, Tesson L, Remy S, Usal C, Osborn MJ, Cost GJ, Bruggemann M, Buelow R and Anegon I (2010) Characterization of immunoglobulin heavy chain knockout rats. *Eur J Immunol* **40**(10):2932-2941.

Miller DS, Bauer B and Hartz AM (2008) Modulation of P-glycoprotein at the blood-brain barrier: opportunities to improve central nervous system pharmacotherapy. *Pharmacol Rev* **60**(2):196-209.

Raub TJ (2006) P-glycoprotein recognition of substrates and circumvention through rational drug design. *Mol Pharm* **3**(1):3-25.

Schinkel AH (1998) Pharmacological insights from P-glycoprotein knockout mice. *Int J Clin Pharmacol Ther* **36**(1):9-13.

Schinkel AH and Jonker JW (2003) Mammalian drug efflux transporters of the ATP binding cassette (ABC) family: an overview. *Adv Drug Deliv Rev* **55**(1):3-29.

Schinkel AH, Smit JJ, van Tellingen O, Beijnen JH, Wagenaar E, van Deemter L, Mol CA, van der Valk MA, Robanus-Maandag EC, te Riele HP and et al. (1994) Disruption of the mouse mdr1a P-glycoprotein gene leads to a deficiency in the blood-brain barrier and to increased sensitivity to drugs. *Cell* **77**(4):491-502.

Schinkel AH, Wagenaar E, Mol CA and van Deemter L (1996) P-glycoprotein in the blood-brain barrier of mice influences the brain penetration and pharmacological activity of many drugs. *J Clin Invest* **97**(11):2517-2524.

Schinkel AH, Wagenaar E, van Deemter L, Mol CA and Borst P (1995) Absence of the mdr1a P-Glycoprotein in mice affects tissue distribution and pharmacokinetics of dexamethasone, digoxin, and cyclosporin A. *J Clin Invest* **96**(4):1698-1705.

Shirasaka Y, Kuraoka E, Spahn-Langguth H, Nakanishi T, Langguth P and Tamai I (2010) Species difference in the effect of grapefruit juice on intestinal absorption of talinolol between human and rat. *J Pharmacol Exp Ther* **332**(1):181-189.

Shirasaka Y, Li Y, Shibue Y, Kuraoka E, Spahn-Langguth H, Kato Y, Langguth P and Tamai I (2009) Concentration-dependent effect of naringin on intestinal absorption of beta(1)-adrenoceptor antagonist talinolol mediated by p-glycoprotein and organic anion transporting polypeptide (Oatp). *Pharm Res* **26**(3):560-567.

Tong C, Li P, Wu NL, Yan Y and Ying QL (2010) Production of p53 gene knockout rats by homologous recombination in embryonic stem cells. *Nature* **467**(7312):211-213.

Trausch B, Oertel R, Richter K and Gramatte T (1995) Disposition and bioavailability of the beta 1-adrenoceptor antagonist talinolol in man. *Biopharm Drug Dispos* **16**(5):403-414.

Urnov FD, Rebar EJ, Holmes MC, Zhang HS and Gregory PD (2010) Genome editing with engineered zinc finger nucleases. *Nat Rev Genet* **11**(9):636-646.

Zhou SF (2008) Structure, function and regulation of P-glycoprotein and its clinical relevance in drug disposition. *Xenobiotica* **38**(7-8):802-832.

Molecular Pharmacology Fast Forward. Published on November 2, 2011 as DOI: 10.1124/mol.111.074179
This article has not been copyedited and formatted. The final version may differ from this version.

Footnotes

Xiaoyan Chu and Zuo Zhang contributed equally to this work.

Molecular Pharmacology Fast Forward. Published on November 2, 2011 as DOI: 10.1124/mol.111.074179
This article has not been copyedited and formatted. The final version may differ from this version.

Figure Legends

Figure 1. Microinjection of *Mdr1a* ZFN mRNA into rat one-cell embryos specifically induces targeted gene mutations. A. Schematic representations of the rat Mdr1a gene structure and the position of the ZFN targeting site selected. The two ZFN binding sequences are shown in opposite orientation in blue and red color, respectively. The ZFN pair consists of two subunits, one with 6 and one with 5 fingers, respectively. When the ZFN pair binds to the target site, the two Fok I domains dimerize to generate a DSB which will be repaired by either NHEJ (major) or HR (minor) pathways. **B.** Screening and analyses of mutant alleles in the rat off-springs derived from ZFN-injected embryos. The positive result in Cel-1 assay indicates that No. 6 and 7 pups may carry mutations near the Mdr1a ZFN target site. The genomic regions surrounding the ZFN site from founder 6 and 7 were cloned and sequenced. Founder 6 contains 4 mutant alleles, with 175, 115, 105 and 11 base pair (bp) deletions, respectively. Founder 7 contains one wild-type allele and 3 mutant alleles with 8, 35 and 19 bp deletions, respectively. The open reading frame of Mdr1a near the ZFN site is shown (1272 amino acids). The deletions that cause frame-shift and translational premature termination are highlighted in red. **C.** Western blot showing undetectable level of Mdr1a protein in the brain and small intestine of KO rats. In the liver sample, the band with an apparently similar size to the Mdr1a protein in KO rats may represent the up-regulated Mdr1b protein due to the cross-reactivity of the antibody. The weak potential Mdr1b protein was detected in the kidney of KO rats as well, but not as strong as in liver.

Molecular Pharmacology Fast Forward. Published on November 2, 2011 as DOI: 10.1124/mol.111.074179
This article has not been copyedited and formatted. The final version may differ from this version.

Figure 2. Brain and plasma concentrations of loperamide and indinavir in Mdr1a$^{-/-}$ and wild-type rats

After intravenous injection of loperamide (1 mg/kg) or indinavir (2 mg/kg), Mdr1a$^{-/-}$ (closed squares) and wild-type rats (open squares) were sacrificed at the indicated time points. The brain and plasma concentrations of loperamide (2A, 2B) and indinavir (2D, 2E) were measured by LC-MS/MS. The brain-to-plasma concentration ratio ($K_{p, brain}$) of loperamide (2C) and indinavir (2F) were also estimated. Values shown are mean ± S.E.

*: Significantly different from wild-type animals ($P<0.05$).

Figure 3. Plasma concentrations of talinolol in Mdr1a$^{-/-}$ and wild-type rats following intravenous and oral administration

Plasma concentration of talinolol in Mdr1a$^{-/-}$ (closed squares) and wild-type rats (open squares) were measured by LC-MS/MS following intravenous (1 mg/kg) (6A) and oral (5 mg/kg) (6B) administration of talinolol. Values shown are mean ± S.E.

Figure 4. Gene expression of various transporters and drug metabolizing enzymes in Mdr1a$^{-/-}$ rat brain, liver, intestine and kidney compared to controls.

From 90 genes tested, the expression of the genes which showed ≥ 2-fold up- or down-regulation (* $P<0.05$) in Mdr1a$^{-/-}$ rats compared to wild-type animals in liver (4A), intestine (4B), kidney (4C), and brain (4D) is presented. The data were expressed as the fold regulation relative to wild-type rats. Fold change greater than 1 indicate up-regulation and the fold regulation is equal to fold change. Fold change less than 1 indicate down-regulation and the fold regulation is the negative inverse of the fold

Molecular Pharmacology Fast Forward. Published on November 2, 2011 as DOI: 10.1124/mol.111.074179
This article has not been copyedited and formatted. The final version may differ from this version.

change. Closed and open bars represent male and female rats, respectively. The data represent mean values of three independent experiments.

Molecular Pharmacology Fast Forward. Published on November 2, 2011 as DOI: 10.1124/mol.111.074179
This article has not been copyedited and formatted. The final version may differ from this version.

Table 1. Pharmacokinetic parameters of talinolol in Mdr1a$^{-/-}$ and wild-type rats following intravenous (1mg/kg) and oral (5mg/kg) administration of talinolol

Parameters	WT (i.v.)	Mdr1a $^{-/-}$ (i.v.)	WT (p.o.)	Mdr1a $^{-/-}$ (p.o.)
AUC/dose (μM.hr/mg/kg)	0.3 ± 0.06	0.4 ± 0.05	0.02 ± 0.002	0.09 ± 0.02*
$T_{1/2}$ (hr)	0.7 ± 0.2	1.0 ± 0.2		
Cl(mL/min/kg)	153 ± 18	119 ± 15		
Vd_{ss} (L/kg)	4.8 ± 0.5	6.5 ± 1.3		
C_{max} (μM)			0.06 ± 0.01	0.21 ± 0.07
T_{max} (hr)			2.0 ± 0.00	1.7 ± 0.3
F (%)			7	23

*: Significantly different from wild-type animals (P<0.05).

Figure 1

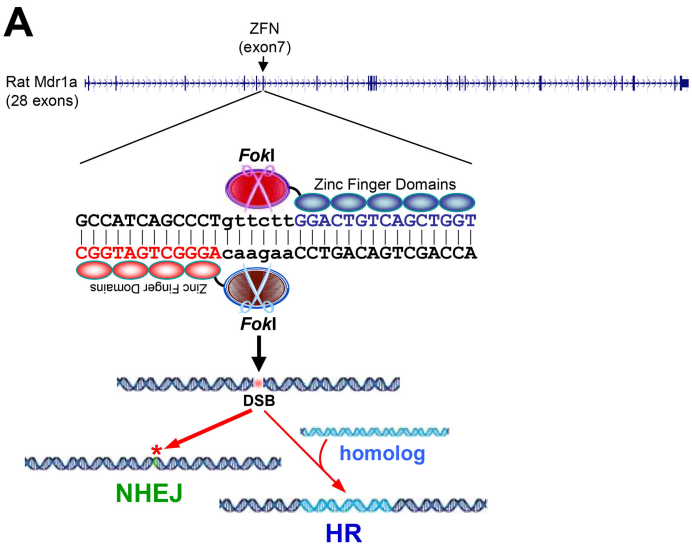

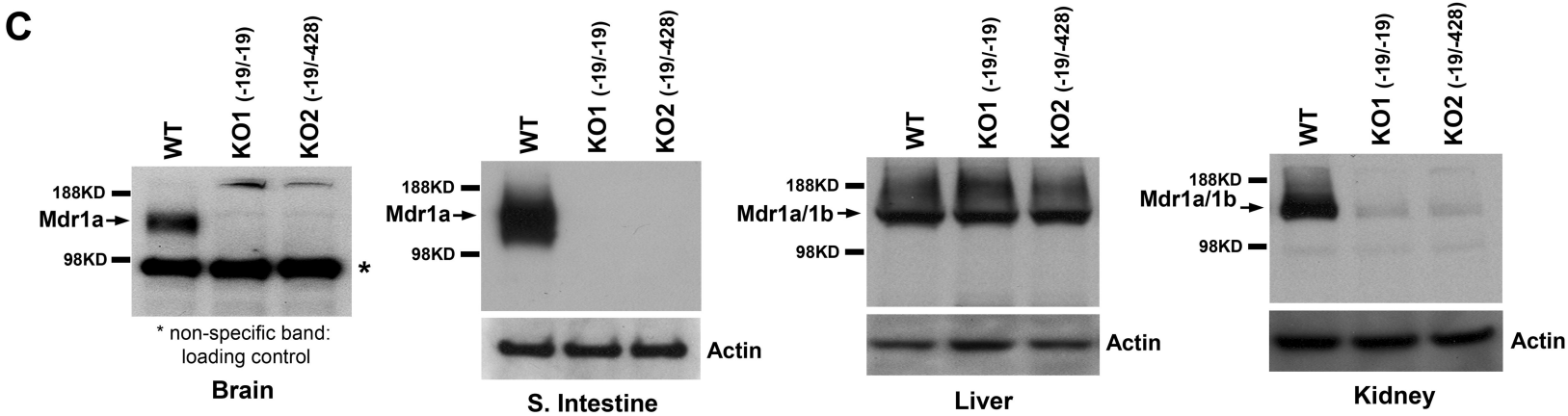

Figure 2

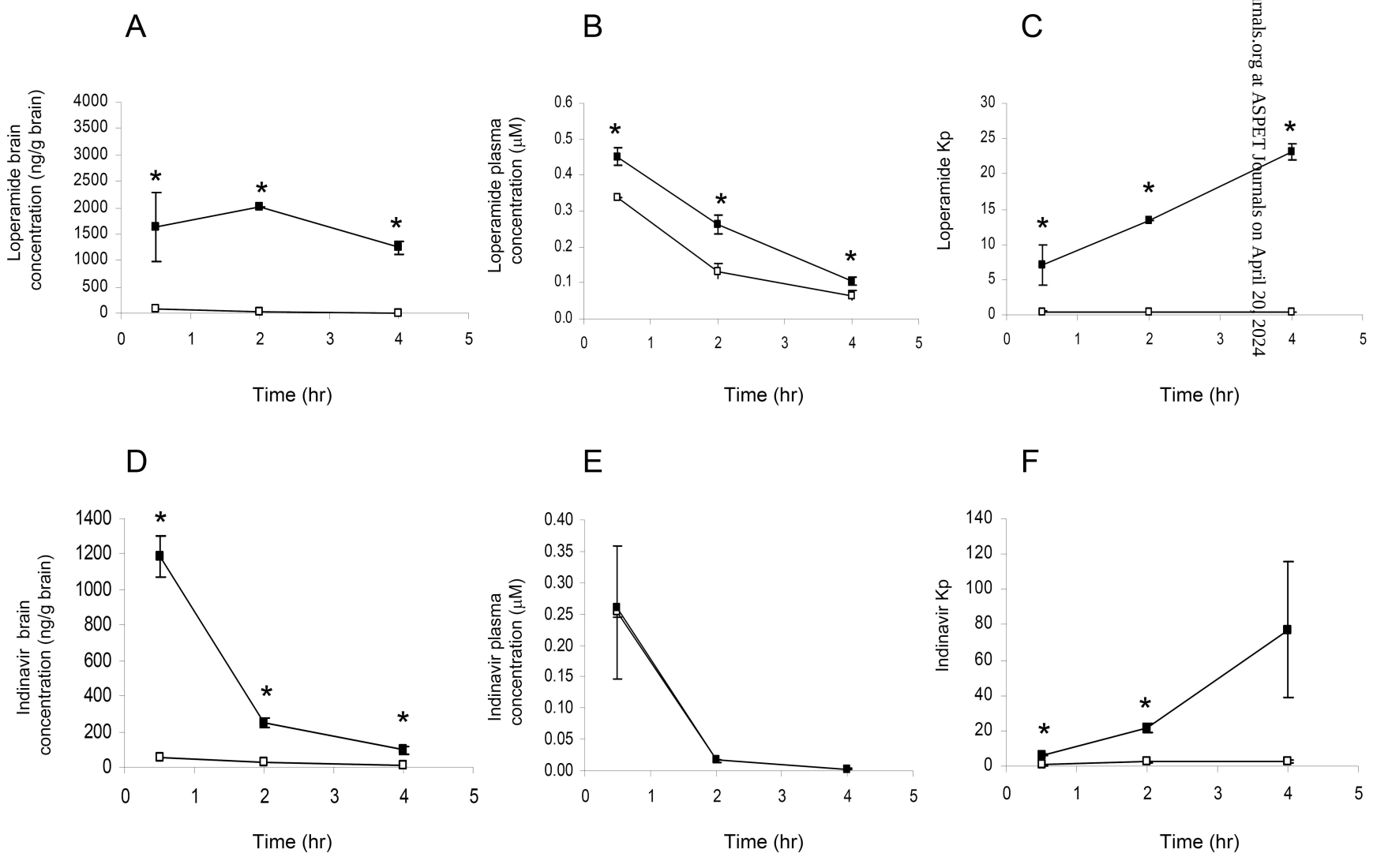

Figure 3

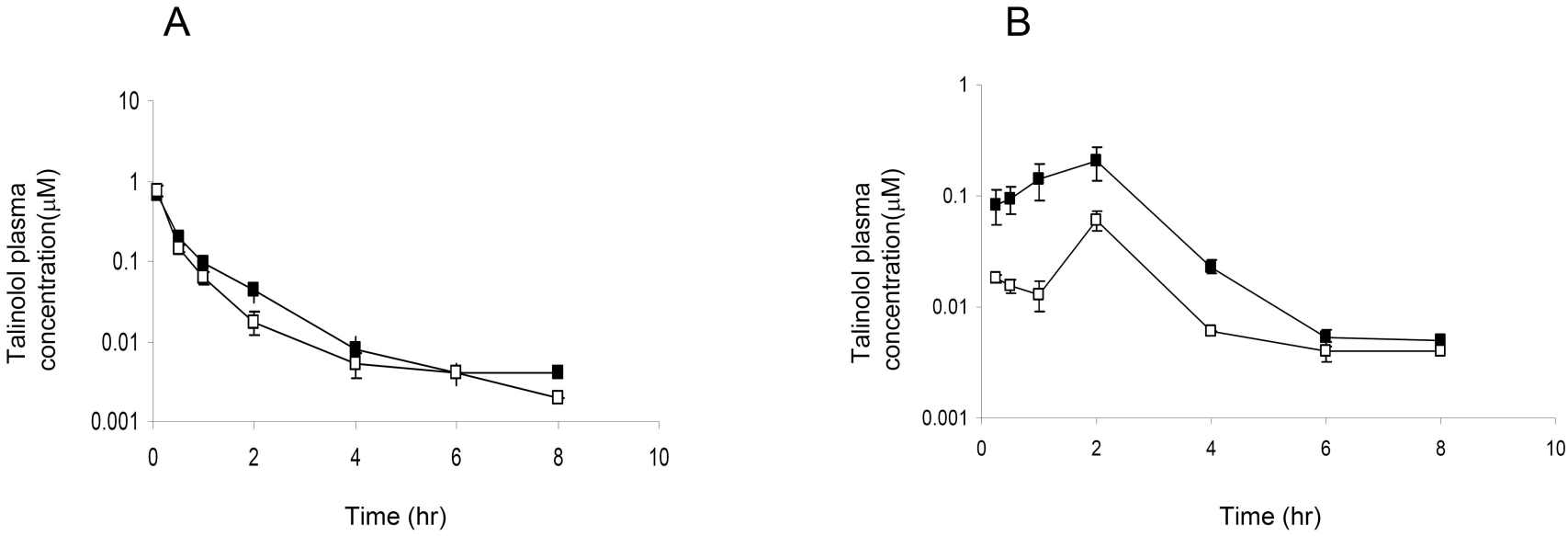

Figure 4

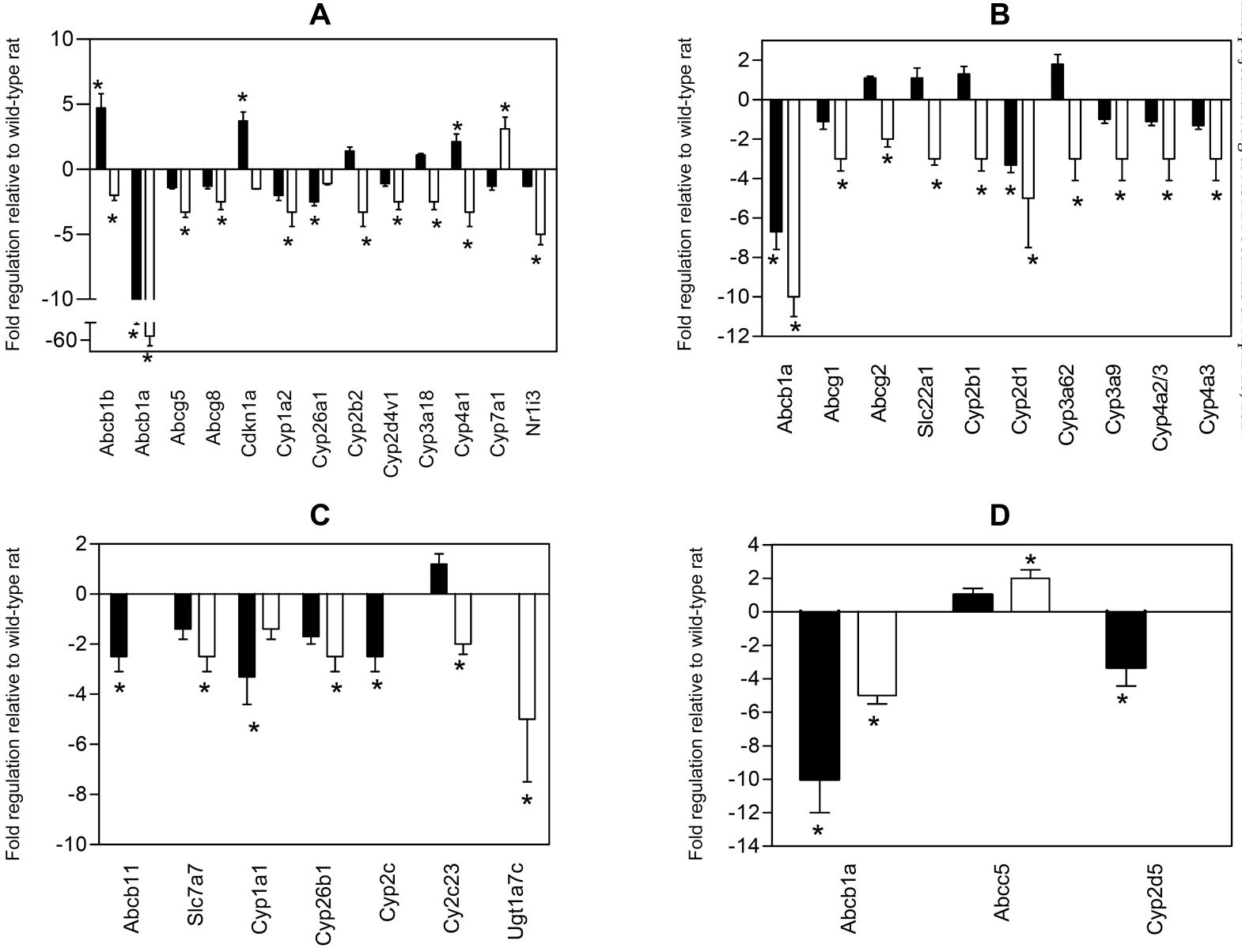
A
Fold regulation relative to wild-type rat
10
5
0
-5
-10
-60
Abcb1b
Abcb1a
Abcg5
Abcg8
Cdkn1a
Cyp1a2
Cyp26a1
Cyp2b2
Cyp2d4v1
Cyp3a18
Cyp4a1
Cyp7a1
Nr1i3
B
Fold regulation relative to wild-type rat
2
0
-2
-4
-6
-8
-10
-12
Abcb1a
Abcg1
Abcg2
Slc22a1
Cyp2b1
Cyp2d1
Cyp3a62
Cyp3a9
Cyp4a2/3
Cyp4a3
C
Fold regulation relative to wild-type rat
2
0
-2
-4
-6
-8
-10
Abcb11
Slc7a7
Cyp1a1
Cyp26b1
Cyp2c
Cy2c23
Ugt1a7c
D
Fold regulation relative to wild-type rat
4
2
0
-2
-4
-6
-8
-10
-12
-14
Abcb1a
Abcc5
Cyp2d5

Supplemental Data

Journal: **Molecular Pharmacology**

Title: **Characterization of Mdr1a/P-glycoprotein knockout rats generated by zinc finger nucleases**

Authors: Xiaoyan Chu, Zuo Zhang, Jocelyn Yabut, Sarah Horwitz, John Levorse, Xiang-qing Li, Lei Zhu, Harmony Lederman, Rachel Ortiga, John Strauss, Xiaofang Li, Karen A. Owens, Jasminka Dragovic, Thomas Vogt, Raymond Evers and Myung Kyun Shin

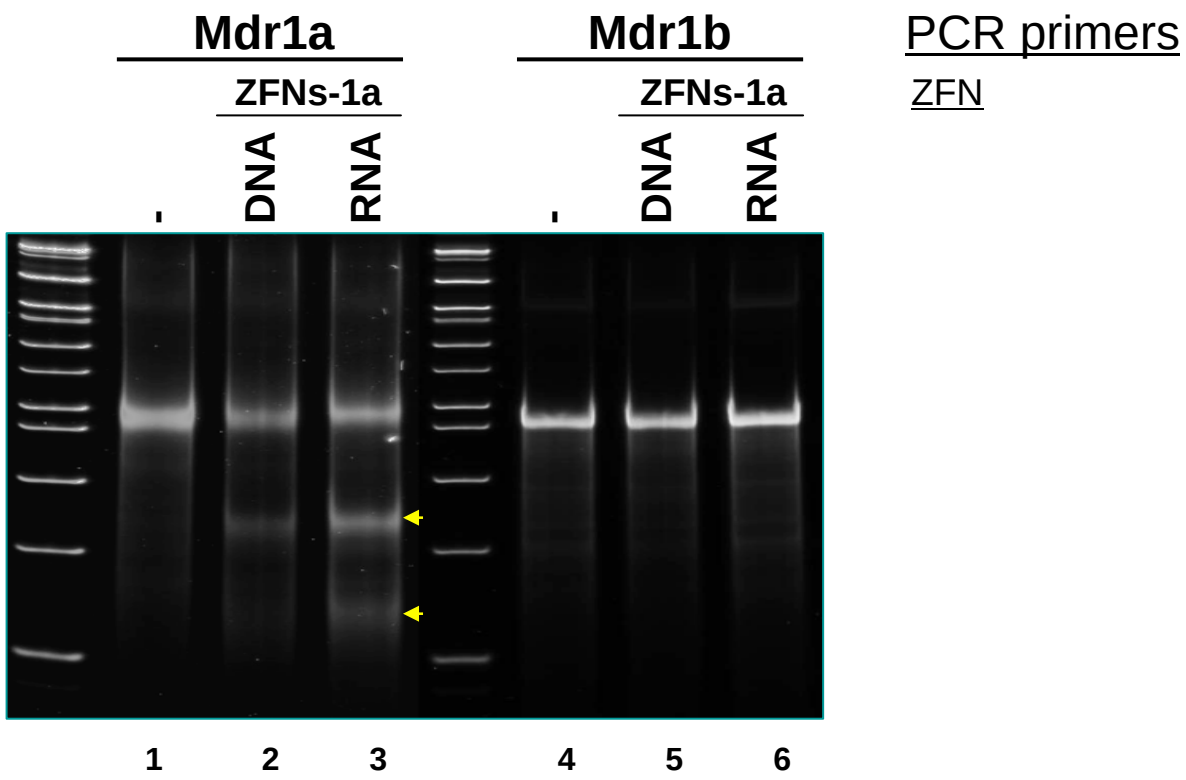

Figure s1. In vitro validation of Mdr1a ZFN in rat C6 cells by Cel-1 assay. Mdr1a-ZFN transfected rat C6 cell genomic DNA was extracted and subjected to PCR using Mdr1a- and Mdr1b-specific primers (Mdr1b-forward: CTGGATAAATTCTGGTTCACAGATCT; Mdr1b-reverse: CTTGGTGGGGCAGAACCATC). The amplified PCR products were analyzed by Cel-1 assay using the Surveyor kit as described in materials and methods. Lane 1&4: transfected with GFP RNA; Lane 2&5: transfected with Mdr1a-ZFN plasmid; Lane 3&6: transfected with Mdr1a ZFN mRNA. The arrows indicate Cel-1 cleaved bands, indicating the functional activity of Mdr1a ZFN.

A

Sites/Chromosomes	Sequences	Mismatches
Mdr1a-ZFN	**GCCATCAGCCCT**gttctt**GGACTGTCAGCTGGT**	0
chr3	GGCCATgAGgCCTCACAAGGgCTcTCAGCTGGTA	4
chr3	AGCCAcCtGCCCTCAGTCaGcCTGcCAGCTGGTG	5
chr8	TGaCATCAGCCCTTGCCAGGACTGctcaCTGGTG	5
chr9	GACCAGCTGACAGTCCTGCCAgaGaCTGAcaGCC	5
chr4	AGCCcTCAGCCCTCGAGATGctCTGTCAtCaGGTG	5
chr14	AGCCAgCAGCCagAGGAGGGACTGgCAGCTGGcC	5
chr12	TaCCcTCAGCCCTCTCATGtACTcTCAGCTGGgG	5
chr7	AACCAGCTttaAcTCCAGCTCTAGGtCTGATGGCT	5
chr7	TGCCATCAGtggTGTGTTtGACTGcCAGCTGGTA	5
chr13	CAgCAtCTcACAaTCCTCTCTGAGaGCTGATGGCA	5
chr2	AACCAcCTGtgAGTCCAGCTCCAGGtCTGATGtCT	5
chr2	TAgtAGCaGAaAGTtCAATCCAGGGCTGATGGCC	5

B

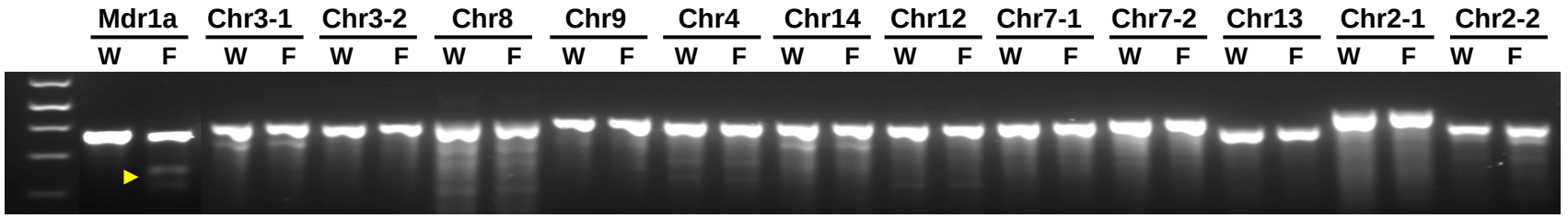

Figure s2. No detectable off-target cleavage detected with Mdr1a ZFN in rat genome. A. 12 sites with 4 or 5 mismatches to the wild-type Mdr1a ZFN site were detected in rat genome. **B.** Each sites from wild-type and founder rats were analyzed by Cel-1 assay using the same Surveyor detection kit. The founder rat No. 6 is shown as an example here. No obvious off-target effect by Mdr1a ZFN was detected in this assay. (W: wild-type rat; F: founder rat)

ZFN Source	Founder ID#	Gender	Deletion/Insertion Size
mRNA	6	F	11, 105, 115 and 175bp deletion, no WT
mRNA	7	F	8, 19, 35bp deletion, and WT
mRNA	23	M	6, 11bp and 428bp deletion, no WT
mRNA	25	F	20bp deletion and WT
mRNA	27	F	6 and 19 deletion, no WT
mRNA	28	F	4bp insertion and 6bp deletion, no WT
mRNA	30	F	19bp deletion. 96+17bp deletion; and WT
mRNA	36	M	11bp deletion and WT
mRNA	40	F	6 and 20bp deletion, no WT
mRNA	41	F	19bp deletion, and WT
mRNA	43	F	11 and 176bp deletion, no WT
mRNA	55	M	6 and 19bp deletion, no WT
mRNA	66	F	6bp deletion, no WT

Table s1. Summary of the genotype of Mdr1a KO founders generated by ZFN injection. All the founders were from ZFN mRNA (2ng/ul) injection. Multiple mutant alleles were easily detected in several founders listed in the last column. No gender bias was observed for founder production.

Table s2. Expression of transporter genes in brain, liver, intestine, and kidney in Mdr1a $^{-/-}$ and wild-type rats

Data are expressed as mean ± SE –fold change in Mdr1a $^{-/-}$ rats compared to wild-type determined from three independent experiments.

Gene	Brain		Liver		Intestine		Kidney	
	Male	Female	Male	Female	Male	Female	Male	Female
Abca1	0.9 ± 0.1	1.5 ± 0.04	0.9 ± 0.1[ce]	0.7 ± 0.1	-[a]	-[a]	0.9 ± 0.1	0.7 ± 0.2[df]
Abcb11	-[b]	-[b]	0.8 ± 0.1	0.7 ± 0.1	-[a]	-[b]	0.4 ± 0.1*[c]	-[a]
Abcb1b	-[a]	-[a]	4.7 ± 1.1*[e]	0.5 ± 0.1*	-[a]	-[a]	1.2 ± 0.4	0.7 ± 0.04[df]
Abcb1a	0.1 ± 0.02*	0.2 ± 0.02*	0.07 ± 0.02*	0.02 ± 0.01*[e]	0.15 ± 0.02*	0.1 ± 0.01*	-[a]	-[a]
Abcb4	1.2 ± 0.4	1.4 ± 0.4	1.0 ± 0.2	0.6 ± 0.1	-[b]	-[a]	-[a]	-[a]
Abcc1	0.7 ± 0.1	1.5 ± 0.1	1.0 ± 0.2	0.7 ± 0.1	0.9 ± 0.04	0.6 ± 0.1	1.0 ± 0.04	0.9 ± 0.1[df]
Abcc2	-[b]	-[b]	1.0 ± 0.1	0.9 ± 0.1	1.1 ± 0.03	1.2 ± 0.3	1.1 ± 0.2	0.7 ± 0.2
Abcc3	-[a]	-[a]	1.1 ± 0.3	0.5 ± 0.1	1.0 ± 0.1	1.0 ± 0.2	1.0 ± 0.2	0.9 ± 0.1[df]
Abcc4	0.8 ± 0.2	1.4 ± 0.5	1.1 ± 0.5[ce]	0.6 ± 0.2	0.7 ± 0.3	1.1 ± 0.8	0.9 ± 0.2	0.6 ± 0.2
	1.2 ± 0.1[g]		1.0 ± 0.6	1.0 ± 0.2	1.2 ± 0.2	0.8 ± 0.2	0.7 ± 0.3	1.1 ± 0.6[df]

Abcc5		1.1 ± 0.3[g]						
Abcc6	0.7 ± 0.2	1.6 ± 0.3	0.8 ± 0.1	0.7 ± 0.2	0.8 ± 0.2[c]	1.6 ± 0.3	0.8 ± 0.1	0.9 ± 0.4 [d]
Abcc8	0.7 ± 0.1	1.7 ± 0.04	-[b]	-[b]	-[b]	-[b]	-[b]	-[b]
Abcg1	0.8 ± 0.3	1.5 ± 0.3	1.4± 0.1 [e]	0.8 ± 0.1	0.9 ± 0.3	0.4. ± 0.1*	0.9 ± 0.3	0.5 ± 0.04
Abcg2	0.9 ± 0.2	0.8 ± 0.1	1.6 ± 0.1	0.9 ± 0.2	1.1 ± 0.1	0.5 ± 0.1*	0.9 ± 0.2[c]	1.0 ± 0.2
Abcg5	-[b]	-[b]	0.7 ± 0.04 [e]	0.3 ± 0.04*	1.4 ± 0.1 [ce]	0.8 ± 0.1	-[b]	-[b]
Abcg8	-[b]	-[b]	0.8 ± 0.1 [e]	0.4 ± 0.1*	1.4 ± 0.4	1.1 ± 0.4	-[b]	-[b]
Slc10a1	-[b]	-[b]	1.1 ± 0.1 [e]	0.5 ± 0.1	-[b]	-[b]	0.7 ± 0.6	-[b]
Slc15a2	1.0 ± 0.2	1.2 ± 0.1	-[b]	-[b]	-[b]	-[b]	0.9 ± 0.1	0.8 ± 0.1 [df]
Slc2a1	-[h]	-[h]	-[h]	-[h]	1.3 ± 0.3[g]	0.7 ± 0.1[g]	-[h]	-[h]
Slc20a2	0.7 ± 0.2	1.2 ± 0.1	0.8 ± 0.1	0.8 ± 0.1	-[a]	-[a]	1.5 ± 0.6[ce]	0.7 ± 0.1
Slc21a4	-[b]	-[b]	-[b]	-[b]	-[b]	-[b]	1.5 ± 0.6	0.8 ± 0.1
Slc22a1	-[b]	-[b]	1.3 ± 0.5	0.6 ± 0.1	1.1 ± 0.5	0.4 ± 0.04*	1.3 ± 0.5[e]	0.5 ± 0.1

Slc22a2	1.4 ± 0.5	-[a]	-[b]	-[b]	-[b]	-[b]	1.0 ±0.2[ce]	0.7 ± 0.3
Slc22a6	1.0 ± 0.1	1.2 ± 0.04	-[b]	-[b]	-[b]	-[b]	0.9 ± 0.2	0.7 ± 0.1
Slc22a7	1.2 ± 0.3	-[b]	1.6 ± 0.1[ce]	0.8 ± 0.04	1.4 ± 0.3	1.5 ± 0.4	0.6 ± 0.1	1.2 ± 0.4[d]
Slc22a8	1.3 ± 0.4	1.0 ± 0.2	2.2 ± 0.8	-[b]	-[b]	-[b]	1.1 ± 0.2	0.7 ± 0.1
Slc29a2	1.0 ± 0.1[g]	0.97 ± 0.3[g]	1.1 ± 0.03[g]	1.0 ± 0.07[g]	-[h]	-[h]	1.2 ± 0.1[g]	1.1 ± 0.1[g]
Slc47a1	1.1 ± 0.1	0.6 ± 0.1	-[b]	-[b]	-[b]	-[b]	1.2 ± 0.5	0.9 ± 0.3
Slc7a7	1.0 ± 0.04	1.7 ± 0.8	1.2 ± 0.1	1.3 ± 0.2	1.1 ± 0.1	0.8 ± 0.1	0.7 ± 0.2	0.4 ± 0.1*
Slco1a1	-[b]	-[b]	1.2 ± 0.5[ce]	0.7 ± 0.2	-[b]	-[b]	1.3 ± 0.3	-[b]
Slco1a4	0.9 ± 0.2	1.3 ± 0.3	1.0 ± 0.1[ce]	0.7 ± 0.2	-[b]	-[b]	-[a]	-[a]
Slco1a5	0.7 ± 0.3	1.4 ± 0.5	0.8 ± 0.3[e]	-[a]	-[b]	-[b]	-[b]	-[b]
Slco1a6	-[b]	-[b]	-[b]	-[b]	-[b]	-[b]	1.1 ± 0.6	0.6 ± 0.1
Slco1b2	-[b]	-[b]	1.4 ± 0.3	0.7 ± 0.2	-[b]	-[b]	-[b]	-[b]
Slco4a1	0.8 ± 0.4	1.7 ± 0.3	-[a]	-[a]	1.0 ± 0.1	1.1 ± 0.3	0.8 ± 0.2[c]	0.7 ± 0.2

* $P < 0.05$ ΔC_t value significantly different from wild-type (wt) rat.

[a] Low gene expression $C_t > 33$.

[b] The gene was not amplified.
[c] Gene expression in wt male was higher than in wt female rats (P<0.05).
[d] Gene expression in wt female was higher than in wt male rats (P<0.05).
[e] Gene expression in Mdr1a knockout (ko) male was higher than in ko female rats (P<0.05).
[f] Gene expression in ko female was higher than in ko male rats (P<0.05).
[g] Beta-actin was used to normalize gene expression.
[h] Expression not tested.

Table S3. Expression of drug metabolism related genes in brain, liver intestine and kidney of Mdr1a $^{-/-}$ and wild-type rats

Data are expressed as mean ± SE –fold change in Mdr1a $^{-/-}$ rats compared to wild-type determined from three independent experiments.

Gene	Brain		Liver		Intestine		Kidney	
	Male	Female	Male	Female	Male	Female	Male	Female
Ahr	1.2 ± 0.2	1.7 ± 0.3	1.2 ± 0.2 [e]	0.7 ± 0.1	1.5 ± 0.3[e]	0.8 ± 0.2	0.9 ± 0.2	1.0 ± 0.1[df]
Atp7b	0.6 ± 0.1	0.7 ± 0.1	0.7 ± 0.1	0.7 ± 0.1	1.0 ± 0.1[c]	1.2 ± 0.4	0.7 ± 0.1	0.5 ± 0.1 [df]
Cdkn1a	-[h]	-[h]	3.7 ± 0.7* [g]	0.7 ± 0.01[g]	-[h]	-[h]	-[h]	-[h]
Cyp17a1	-[b]	-[b]	0.8 ± 0.1	0.9 ± 0.2 [df]	1.3 ± 0.3	1.1 ± 0.4	-[a]	-[a]
Cyp1a1	-[b]	-[b]	1.2 ± 0.6 [e]	-[a]	0.5 ± 0.3	1.9 ± 0.6	0.3 ± 0.1*	0.7 ± 0.2 [d]
Cyp1a2	-[b]	-[b]	0.5 ± 0.1	0.3 ± 0.1*	-[b]	-[b]	-[b]	-[b]
Cyp26a1	1.7 ± 0.7	1.4 ± 0.6	0.4 ± 0.04*	0.9 ± 0.1 [df]	-[b]	-[b]	0.6 ± 0.1	0.7 ± 0.2
Cyp26b1	0.5 ± 0.1	1.2 ± 0.5	0.7 ± 0.1[ce]	-[a]	-[a]	-[b]	0.6 ± 0.1	0.4 ± 0.1*
Cyp2a1	-[b]	-[b]	0.9 ± 0.1	0.8 ± 0.1[d]	-[b]	-[b]	-[b]	-[b]
Cyp2a2	-[b]	-[b]	1.1 ± 0.2[ce]	1.5 ± 0.4	-[b]	-[b]	-[b]	-[b]
Cyp2b1	-[b]	-[b]	0.8 ± 0.1	0.2 ± 0.1	1.3 ± 0.4[e]	0.4 ± 0.1*	-[b]	1.5 ± 0.5

Cyp2b2	-[b]	-[b]	1.4 ± 0.3 [c]	0.3 ± 0.1*	-[b]	-[b]	-[b]	1.5 ± 0.5
Cyp2b3	-[b]	-[b]	0.8 ± 0.1	1.6 ± 0.01	-[b]	-[a]	-[b]	-[b]
Cyp2c12	-[b]	-[b]	1.6 ± 0.4	0.9 ± 0.2	-[b]	-[b]	-[b]	-[b]
Cyp2c13	-[b]	-[b]	1.3 ± 0.1[ce]	-[a]	-[b]	-[b]	-[b]	-[b]
Cyp2c22	-[b]	-[b]	1.7 ± 0.2[ce]	0.6 ± 0.1	-[b]	-[b]	-[b]	-[b]
Cyp2c23	-[b]	-[b]	0.9 ± 0.2	0.8± 0.2	-[b]	-[a]	1.2 ± 0.4	0.5 ± 0.1[*]
Cyp2c37	-[b]	-[b]	1.4 ± 0.1[ce]	-[a]	-[a]	-[a]	- [b]	-[b]
Cyp2c7	-[a]	-[b]	0.9 ± 0.1	0.6 ± 0.1[d]	-[b]	-[b]	-[b]	-[b]
Cyp2c	-[b]	-[b]	1.2 ± 0.3 [ce]	-[a]	-[b]	-[b]	0.4 ± 0.1*	-[b]
Cyp2d1	-[a]	-[a]	-[b]	0.7 ± 0.3	0.3 ±0.04*	0.2 ±0.1*[df]	1.1 ± 0.7[c]	0.6 ± 0.2
Cyp2d2	-[b]	-[b]	0.9 ± 0.1[e]	0.7 ± 0.1	0.8 ± 0.1	1.1 ± 0.4	0.7 ± 0.1	0.8 ± 0.2
Cyp2d3	-[b]	-[b]	1.1 ± 0.1 [ce]	0.8 ± 0.1	-[a]	0.8 ± 0.1	-[b]	-[b]
Cyp2d4v1	0.8 ± 0.2	1.1 ± 0.2	0.9 ± 0.2 [e]	0.4 ± 0.1*[df]	1.2 ± 0.02	0.7 ± 0.1	0.9 ± 0.2 [ce]	0.5 ± 0.2
Cyp2d5	0.3 ± 0.1 *	-[b]	1.9 ± 0.5 [e]	0.8 ± 0.2	0.9 ± 0.03	0.8 ± 0.2	1.3 ± 0.1 [ce]	0.8 ± 0.3
Cyp2e1	-[a]	-[b]	0.7 ± 0.02	0.6 ± 0.2	-[b]	-[b]	1.3 ± 0.5	0.6 ± 0.2[d]
Cyp3a18	-[b]	-[b]	1.1 ± 0.1 [ce]	0.4 ± 0.1*	0.8 ± 0.2	0.7 ± 0.2	-[b]	-[b]
Cyp3a23/3a1	-[b]	-[b]	1.5 ± 0.3 [ce]	0.6 ± 0.1	-[b]	-[b]	-[b]	-[b]
Cyp3a11	-[b]	-[b]	1.2 ± 0.4 [ce]	-[a]	-[b]	-[b]	-[b]	-[b]
Cyp3a62	-[a]	1.2 ± 0.5	1.6 ± 0.4 [ce]	0.8 ± 0.1	1.8 ± 0.5[e]	0.3 ± 0.1*	-[b]	-[b]

Cyp3a9	0.8 ± 0.04	1.4 ± 0.3	0.8 ± 0.05	0.8 ± 0.2[df]	1.0 ± 0.2[e]	0.3 ± 0.1*	-[b]	-[b]
Cyp4a1	-[b]	-[b]	2.1 ± 0.6*	0.3 ± 0.1*[d]	0.9 ± 0.2	0.6 ± 0.04	1.0 ± 0.3	0.6 ± 0.1[df]
Cyp4a2;Cyp4a3	-[a]	-[b]	1.3 ± 0.2[ce]	0.5 ± 0.1	0.9 ± 0.2	0.3 ± 0.1*[d]	1.0 ± 0.4[ce]	0.7 ± 0.2
Cyp4a3	-[b]	-[b]	1.2 ± 0.2[ce]	0.5 ± 0.1	0.8± 0.1	0.3 ± 0.1*	0.7 ± 0.2	0.7 ± 0.2
Cyp4a8	-[b]	-[b]	0.6 ± 0.1[ce]	-[a]	-[b]	-[b]	1.2 ± 0.4	0.7 ± 0.1[df]
Cyp7a1	-[b]	-[b]	0.8 ± 0.2[c]	3.1 ± 0.9*	-[b]	-[b]	-[b]	-[b]
Gsta2	-[b]	-[b]	1.0 ± 0.1[ce]	0.9 ± 0.4	0.6 ± 0.2	2.4 ± 0.7	1.7 ± 0.6[c]	0.9 ± 0.4
Gstm1	0.8 ± 0.3	1.4 ± 0.2	1.1 ± 0.1[ce]	0.6 ± 0.1	0.8 ± 0.2	0.4 ± 0.2	0.7 ± 0.1	0.6 ± 0.2[d]
Gstm2	0.6 ± 0.1	1.6 ± 0.2	0.9 ± 0.2[ce]	0.6 ± 0.2	0.6 ± 0.1[c]	1.6± 0.1	0.7 ± 0.1	0.6 ± 0.1[d]
Gstm7	1.1 ± 0.1	1.4 ± 0.1	0.6 ± 0.04[ce]	0.6 ± 0.1	-[a]	-[a]	1.0 ± 0.4	0.7 ± 0.1[d]
Gstp1	0.9 ± 0.4	1.1 ± 0.1	0.8 ± 0.04[c]	0.7 ± 0.1	1.0 ± 0.3[ce]	1.3 ± 0.4	1.1 ± 0.3	0.9 ± 0.1
Gstt1	0.9 ± 0.2	1.1 ± 0.2	0.8 ± 0.1	0.8 ± 0.1	1.0 ± 0.2	1.6 ± 0.6	1.0 ± 0.3	0.7 ± 0.1[d]
Hnmt	1.5 ± 0.5[g]	1.0 ± 0.5[g]	-[h]	-[h]	0.7 ± 0.4[g]	3.9 ± 1.1[g]	-[h]	-[h]

Inmt	-[h]	-[h]	0.86 ± 0.7 [g]	0.5 ± 0.1* [g]	-[h]	-[h]	-[h]	-[h]
Nr1i2	-[b]	-[a]	0.9 ± 0.1 [e]	0.6 ± 0.1	1.0 ± 0.1[c]	1.2 ± 0.2	0.5 ± 0.04	0.9 ± 0.1 [f]
Nr1i3	-[b]	-[b]	0.8 ± 0.01 [e]	0.2 ± 0.03*	1.2 ± 0.2[e]	0.7 ± 0.1	-[b]	-[a]
Sult1a1	0.8 ± 0.2	1.0 ± 0.2	0.9 ± 0.1 [ce]	0.5 ± 0.1	-[a]	-[a]	1.2 ± 0.4	0.7 ± 0.1
Sult1b1	-[b]	-[b]	1.2 ± 0.3	0.6 ± 0.1[d]	1.0 ± 0.2	1.1 ± 0.4	1.1 ± 0.4	0.5 ± 0.1
Sult1c3	-[b]	-[b]	1.1 ± 0.1 [ce]	1.0 ± 0.1	-[b]	-[b]	1.7 ± 0.2	1.8 ± 0.2 [d]
Ugt1a1	-[b]	-[b]	0.9 ± 0.03 [e]	0.6 ± 0.1	0.8 ± 0.1[ce]	0.6 ± 0.1	0.9 ± 0.2	0.6 ± 0.1
Ugt1a6	0.8 ± 0.4	0.7 ± 0.2	0.7 ± 0.1[c]	0.7 ± 0.2	1.3 ± 0.3	1.3 ± 0.3	0.9 ± 0.3	0.6 ± 0.1 [df]
Ugt1a7c	-[a]	-[a]	1.2 ± 0.9	0.8 ± 0.4	0.8 ± 0.2	0.9 ± 0.4	-[b]	0.2 ± 0.1* [d]
Ugt1a8	0.8 ± 0.1	1.5 ± 0.3	0.8 ± 0.2	0.9 ± 0.3 [d]	1.1 ± 0.2	1.5 ± 0.6	0.8 ± 0.3	0.5 ± 0.1[df]
Ugt2b17	-[b]	-[b]	0.6 ± 0.1	0.6 ± 0.2	-[b]	-[b]	-[b]	-[b]
Ugt2b36	-[b]	-[b]	1.0 ± 0.1	0.8 ± 0.3	2.2 ± 0.6	1.7 ± 0.1	0.8 ± 0.3	1.0 ± 0.2
Ugt2b	-[b]	-[b]	1.4 ± 0.3	0.6 ± 0.2 [d]	-[b]	-[b]	-[b]	-[b]

* $P < 0.05$ ΔC_t value significantly different from wild-type (wt) rat.
[a] Low gene expression $C_t > 33$.
[b] The gene was not amplified.
[c] Gene expression in wt male was higher than in wt female rats ($P<0.05$).
[d] Gene expression in wt female was higher than in wt male rats ($P<0.05$).
[e] Gene expression in Mdr1a knockout (ko) male was higher than in ko female rats ($P<0.05$).
[f] Gene expression in ko female was higher than in ko male rats ($P<0.05$).
[g] Beta-actin was used to normalize gene expression.
[h] Expression not tested.

Table S4. Gene list of SABioscience's 384-well PCR arrays (preliminary data available upon request)

Position	Gene Symbol
1	Abca1
2	Abca13
3	Abca17
4	Abca2
5	Abca3
6	Abca4
7	Abca9
8	Abcb11
9	Abcb1b
10	Abcb4
11	Abcb5
12	Abcb6
13	Abcc1
14	Abcc10
15	Abcc12
16	Abcc2
17	Abcc3
18	Abcc4
19	Abcc5
20	Abcc6
21	Abcd1
22	Abcd3
23	Abcd4
24	Abcf1
25	Abcg2
26	Abcg8
27	Aqp1
28	Aqp7
29	Aqp9
30	Atp6v0c
31	Atp7a
32	Atp7b
33	Mvp
34	Slc10a1
35	Slc10a2
36	Slc15a1
37	Slc15a2
38	Slc16a1
39	Slc16a2
40	Slc16a3
41	Slc19a1
42	Slc19a2
43	Slc19a3
44	Slc22a1
45	Slc22a2
46	Slc22a3

47	Slc22a6
48	Slc22a7
49	Slc22a8
50	Slc22a9
51	Slc25a13
52	Slc28a1
53	Slc28a2
54	Slc28a3
55	Slc29a1
56	Slc29a2
57	Slc2a1
58	Slc2a2
59	Slc2a3
60	Slc31a1
61	Slc38a2
62	Slc38a5
63	Slc3a1
64	Slc3a2
65	Slc5a1
66	Slc5a4a
67	Slc7a11
68	Slc7a4
69	Slc7a5
70	Slc7a6
71	Slc7a7
72	Slc7a8
73	Slc7a9
74	Slco1a5
75	Slco1a6
76	Slco1b2
77	Slco2a1
78	Slco2b1
79	Slco3a1
80	Slco4a1
81	Tap1
82	Tap2
83	Vdac1
84	Vdac2
85	Aadac
86	Adh1
87	Adh4
88	Adh6
89	Adh7
90	Aldh1a1
91	Aldh1a2
92	Aldh1a3
93	Aldh1b1
94	Aldh2
95	Aldh3a1
96	Aldh3a2

97	Aldh3b1
98	Aldh3b2
99	Aldh5a1
100	Aldh6a1
101	Aldh7a1
102	Aldh8a1
103	Aldh9a1
104	Cel
105	Cyp11a1
106	Cyp11b1
107	Cyp17a1
108	Cyp19a1
109	Cyp1a1
110	Cyp1a2
111	Cyp1b1
112	Cyp24a1
113	Cyp26a1
114	Cyp26b1
115	Cyp26c1
116	Cyp27a1
117	Cyp27b1
118	Cyp2a3a
119	Cyp2c
120	Cyp2c22
121	Cyp2c23
122	Cyp2c37
123	Cyp2c6
124	Cyp2c7
125	Cyp2c80
126	Cyp2d2
127	Cyp2d4v1
128	Cyp2e1
129	Cyp2f4
130	Cyp2r1
131	Cyp2s1
132	Cyp2t1
133	Cyp2w1
134	Cyp3a18
135	Cyp3a23/3a1
136	Cyp3a9
137	Cyp4a1
138	Cyp4a3
139	Cyp4a8
140	Cyp4b1
141	Cyp4f1
142	Cyp4f18
143	Cyp4f4
144	Cyp4f40
145	Cyp4f6
146	Cyp7a1

147 Cyp7b1
148 Cyp8b1
149 Dhrs2
150 Dpyd
151 Esd
152 Fmo1
153 Fmo2
154 Fmo3
155 Fmo4
156 Fmo5
157 Gzma
158 Gzmb
159 Hsd17b10
160 Maob
161 Ptgs1
162 Ptgs2
163 Tas1r2
164 Uchl1
165 Uchl3
166 Xdh
167 A3galt2
168 A4galt
169 Aanat
170 Acsl1
171 Acsl3
172 Acsl4
173 Acsm3
174 Agxt
175 Alg5
176 As3mt
177 Asmt
178 Baat
179 Ccbl1
180 Es22
181 Ces2
182 Ces3
183 Ces7
184 Chst7
185 Comt
186 Ddost
187 Eef1b2
188 Ephx1
189 Ephx2
190 Galnt1
191 Galnt3
192 Galnt4
193 Gamt
194 Gcnt1
195 Gcnt2
196 Glyat

197	Gnmt
198	Gsta2
199	Gsta3
200	Gsta4
201	Gstk1
202	Gstm1
203	Gstm2
204	Gstm4
205	Gstm5
206	Gsto1
207	Gsto2
208	Gstp1
209	Gstt1
210	Gstt2
211	Has1
212	Hnmt
213	Inmt
214	Mgat1
215	Mgat2
216	Mgst1
217	Mgst2
218	Mgst3
219	Nat1
220	Nat2
221	Nqo1
222	Nqo2
223	Pnmt
224	Pomgnt1
225	Ptges
226	Ptges2
227	Gstt3
228	Sult1a1
229	Sult1b1
230	Sult1c3
231	Sult1c2
232	Sult1e1
233	Sult2a1
234	Sult2b1
235	Sult4a1
236	Sult5a1
237	Tst
238	Ugt2b17
239	Ugcg
240	Ugt1a1
241	Ugt1a5
242	Ugt1a6
243	Ugt1a8
244	Ugt1a9
245	Ugt2a1
246	Ugt2b

247 Ugt2b5
248 Ugt8
249 Abcb1
250 Ahr
251 Ap1s1
252 Apc
253 Ar
254 Arnt
255 Atm
256 Bax
257 Bcl2
258 Bcl2l1
259 Blmh
260 Brca1
261 Brca2
262 Ccnd1
263 Ccne1
264 Cdk2
265 Cdk4
266 Cdkn1a
267 Cdkn1b
268 Cdkn2a
269 Cdkn2d
270 Crabp1
271 Cyp2b2
272 Cyp2c13
273 Cyp2c79
274 Cyp3a2
275 Dhfr
276 Egfr
277 Elk1
278 Erbb2
279 Erbb3
280 Erbb4
281 Ercc3
282 Esr1
283 Esr2
284 Fgf2
285 Fos
286 Gabpa
287 Hif1a
288 Igf2r
289 Mafb
290 Met
291 Myc
292 Nfkb1
293 Nfkb2
294 Nfkbib
295 Nfkbie
296 Ppara

297	Ppard
298	Pparg
299	Rara
300	Rarb
301	Rxra
302	Rxrb
303	Sod1
304	Top1
305	Top2a
306	Top2b
307	Tp53
308	Xpa
309	Xpc
310	Abcc8
311	Abcg1
312	Abcg5
313	Slc20a2
314	Slc21a4
315	Slc47a1
316	Slco1a1
317	Cyp2a1
318	Cyp2a2
319	Cyp2b1
320	Cyp2b3
321	Cyp2c12
322	Cyp2d1
323	Cyp2d3
324	Cyp3a62
325	Nr1i2
326	Nr1i3
327	Ugt1a7c
328	Ugt2b36
329	Slco1a4
330	Abca5
331	ABCA7
332	Abcb10
333	abcb7
334	Abcb8
335	Abcb9
336	Abcc9
337	Abcd2
338	Abce1
339	Abcf3
340	Abcg3l2
341	Abcg4
342	Adh6a
343	Adhfe1
344	Aip
345	Aldh16a1
346	Aldh1a7

347 Aldh1l1
348 Aldh1l2
349 Aox1
350 Cyp11b3
351 Cyp20a1
352 Cyp2b15
353 Cyp2b21
354 Cyp2j10
355 Cyp2j3
356 Cyp2j4
357 Cyp2u1
358 Cyp39a1
359 Cyp46a1
360 Cyp4v3
361 Cyp4x1
362 Cyp51
363 Gstcd
364 Gstm6
365 Hnf4a
366 Kynu
367 LOC310902
368 Ugt1a2
369 Ugt1a3
370 Ugt2a3
371 Ugt2b34
372 Gstm7
373 Rplp1 – internal control
374 Hprt1 – internal control
375 Rpl13a – internal control
376 Ldha – internal control
377 Actb – internal control
378 RGDC – DNA contamination control
379 RTC – RT control
380 RTC – RT control
381 RTC – RT control
382 PPC – PCR control
383 PPC – PCR control
384 PPC – PCR control

Figure S3. SABioscience PCR array Volcano Plot (detailed preliminary data available upon request)

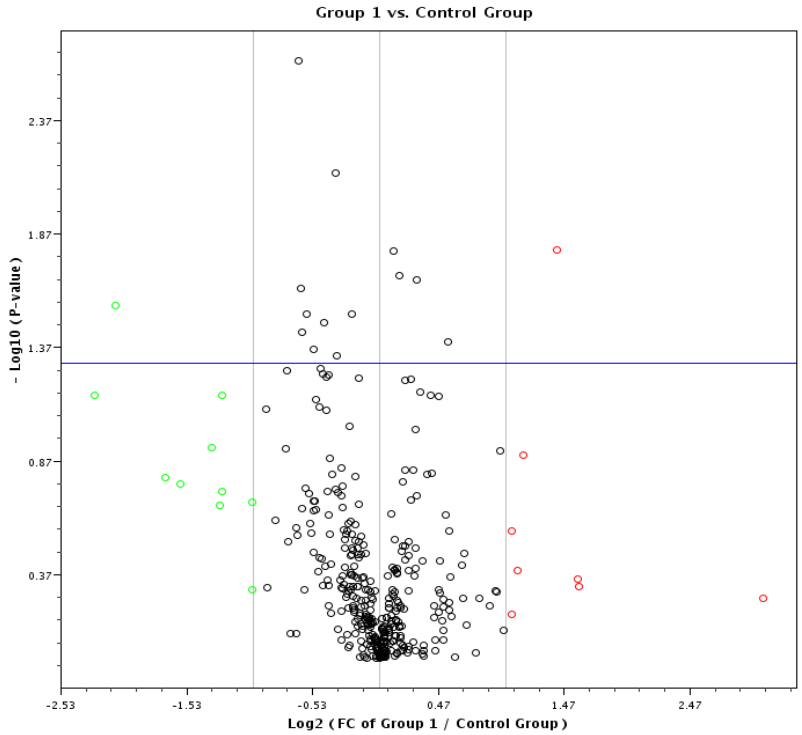

Kidney Male KO vs. WT

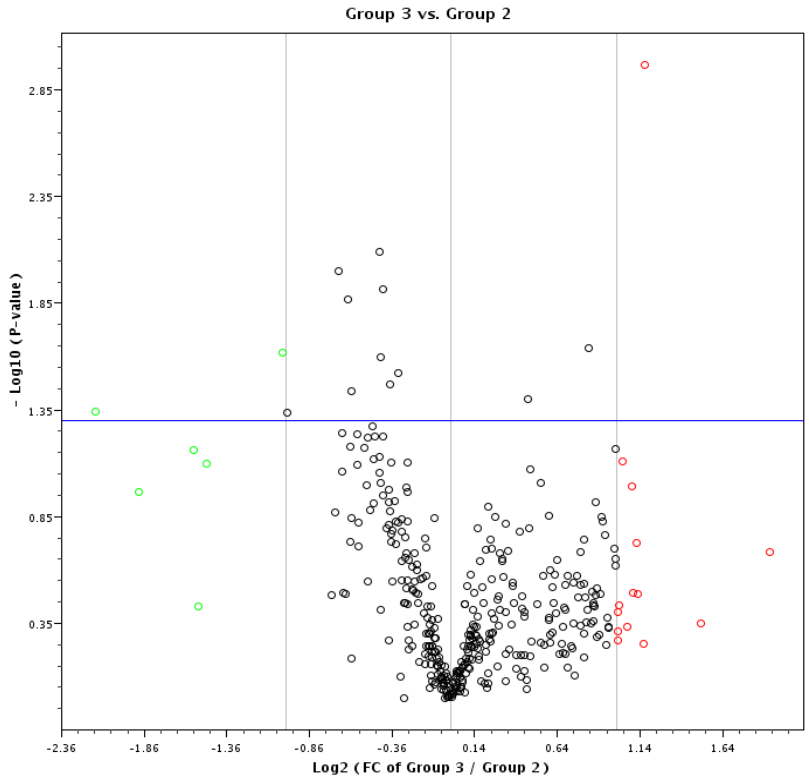

Kidney Female KO vs. WT

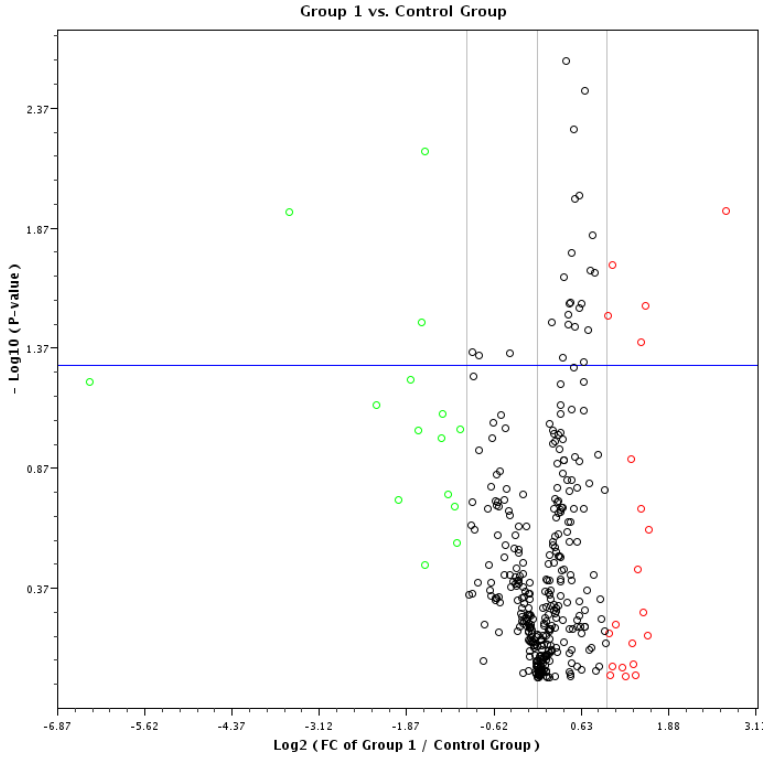

Liver Male KO vs. WT

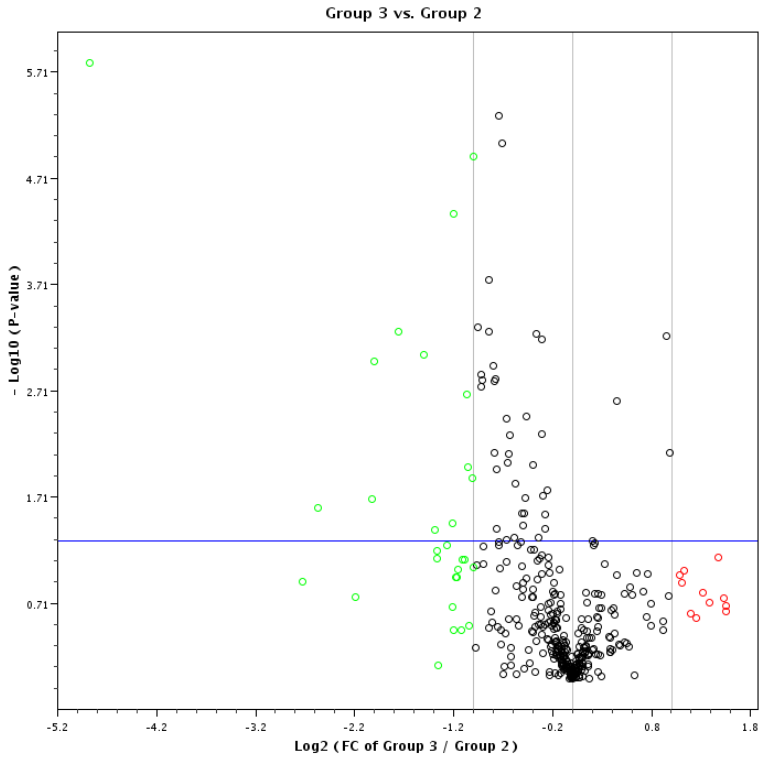

Liver Female KO vs. WT

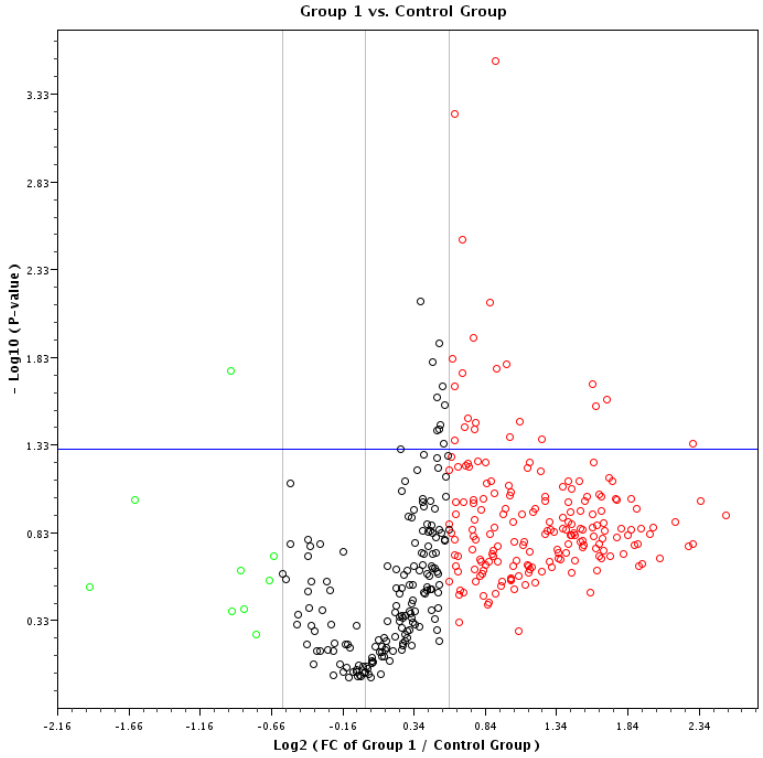

Intestine Male KO vs. WT

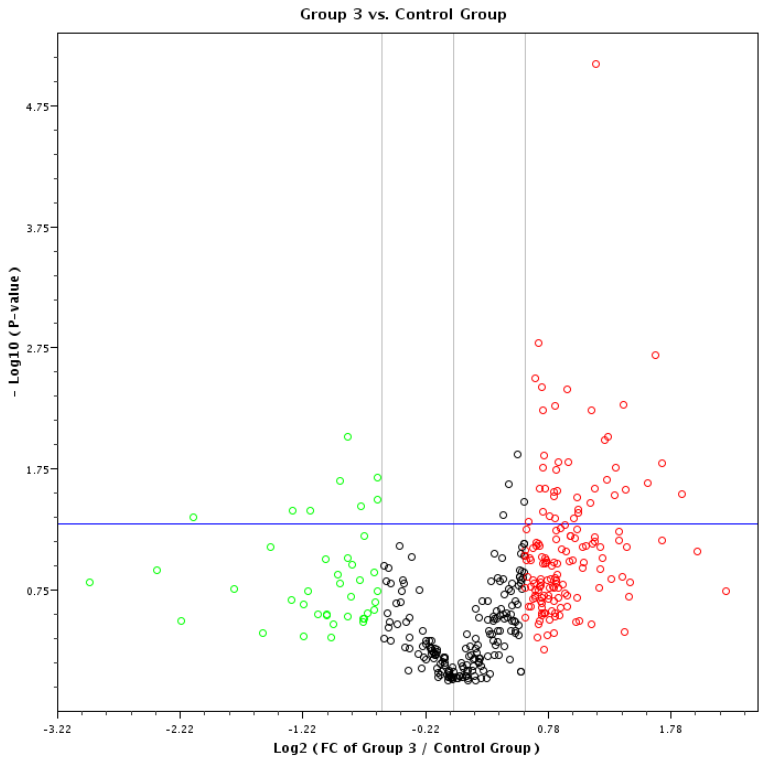

Intestine Female KO vs. WT

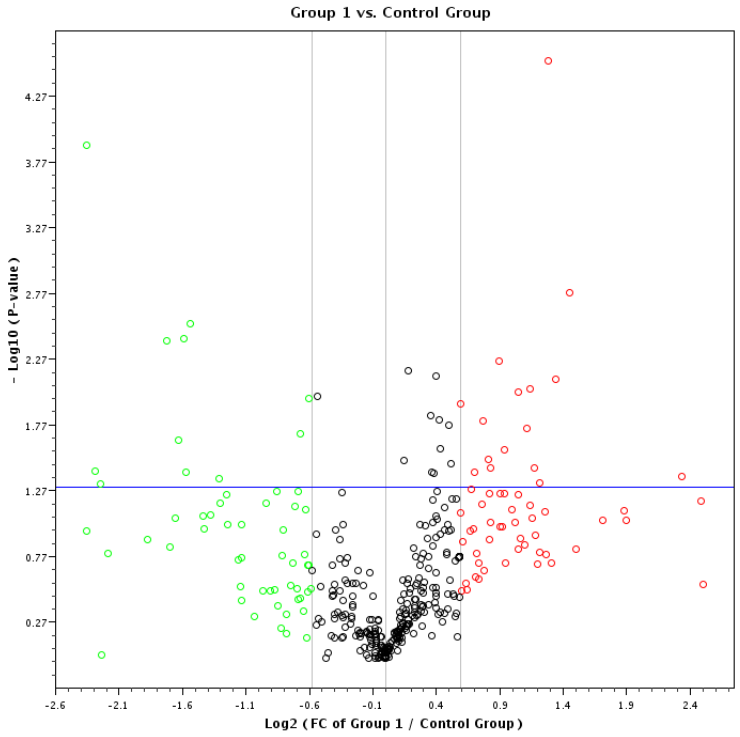

Brain Male KO vs. WT

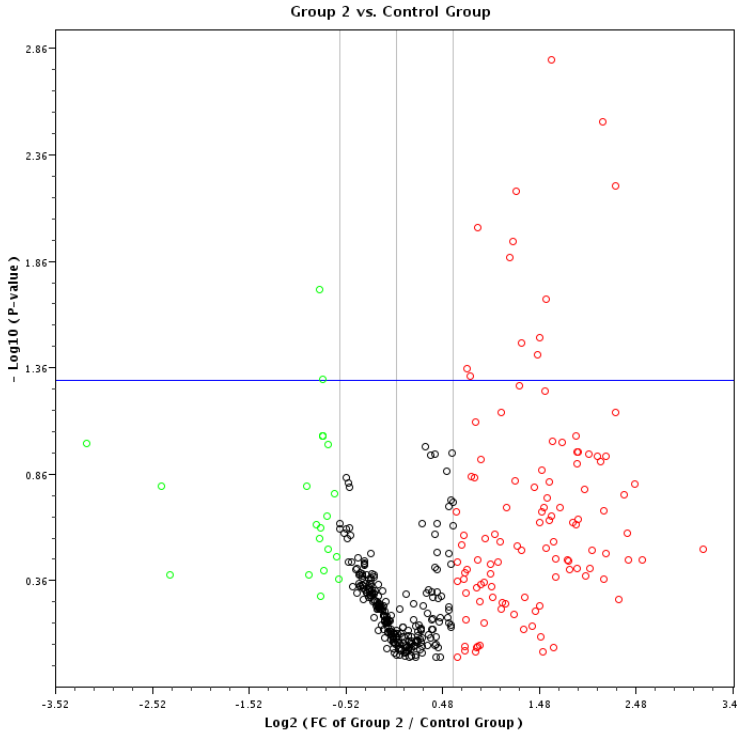

Brain Female KO vs. WT